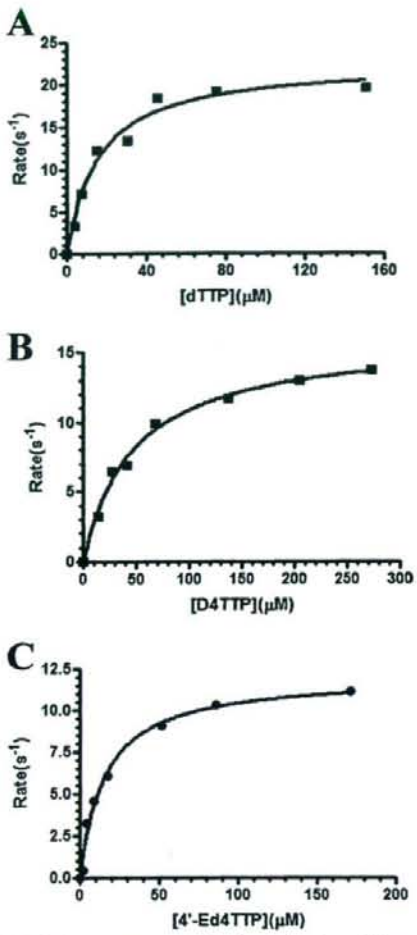

FIG. 3. Single-turnover assays for determination of K_d and k_{pol} of dTMP, d4TMP, and 4′-Ed4TMP incorporation by wt RT. (A) The observed rates of dTMP incorporation into the 23-/36-mer DNA/DNA P/T by wt RT were plotted against dTTP concentration to give a dissociation constant (K_d) of 15.4 ± 2.9 μM and a maximum rate of incorporation (k_{pol}) of 22.6 ± 1.3 s^{-1}. (B) The observed rates of d4TMP incorporation into the 23-/36-mer DNA/DNA P/T by wt RT were plotted against d4TTP concentration to give a K_d of 48.0 ± 4.8 μM and a k_{pol} of 16.0 ± 0.5 s^{-1}. (C) The observed rates of 4′-Ed4TMP incorporation into the 23-/36-mer DNA/DNA P/T by wt RT were plotted against 4′-Ed4TTP concentration to give a K_d of 15.8 ± 2.4 μM and a k_{pol} of 12.1 ± 0.5 s^{-1}.

dTMP incorporation at 1.47 μM^{-1} s^{-1}, consistent with the previously reported values (18, 35). The k_{pol} value for d4TTP is 16 s^{-1}, similar to that for dTTP, while the K_d value for d4TTP is 48.0 μM, about threefold higher than that for dTTP. Hence, the efficiency of d4TMP incorporation is 0.33 μM^{-1} s^{-1}, which is about fourfold lower than that of dTTP. On the other hand, the K_d value for 4′-Ed4TTP is 15.8 μM, the same as that for dTTP, but threefold lower than that for its parental compound d4TTP. The k_{pol} value for 4′-Ed4TTP is 12 s^{-1}, slightly less than those for dTTP

TABLE 3. Pre-steady-state kinetic parameters for dTMP, d4TMP, and 4′-Ed4TMP incorporation by wt RT and the M184V mutant with DNA/DNA and DNA/RNA P/Ts

P/T	Enzyme	dTTP			d4TTP				4′-Ed4TTP			
		K_d(μM) (mean ± SD)	k_{pol}(s^{-1}) (mean ± SD)	k_{pol}/K_d (μM^{-1} s^{-1})	K_d(μM) (mean ± SD)	k_{pol}(s^{-1}) (mean ± SD)	k_{pol}/K_d (μM^{-1} s^{-1})	Selectivity[a]	K_d(μM) (mean ± SD)	k_{pol}(s^{-1}) (mean ± SD)	k_{pol}/K_d (μM^{-1} s^{-1}) (mean ± SD)	Selectivity[a]
DNA/DNA	wt RT	15.4 ± 2.9	22.6 ± 1.3	1.47	48.0 ± 4.8	16.0 ± 0.5	0.33	4.5	15.8 ± 2.4	12.1 ± 0.5	0.77	1.9
	M184V	73.2 ± 8.0	22.4 ± 0.9	0.31	605 ± 285	29.8 ± 10.4	0.05	6.2	168.1 ± 25.6	18.9 ± 1.1	0.11	2.8
DNA/RNA	wt RT	67.1 ± 10.2	65.0 ± 3.9	0.97	40.8 ± 9.2	18.4 ± 1.4	0.45	2.2	11.4 ± 2.7	11.7 ± 0.8	1.0	0.97
	M184V	143.9 ± 25.0	41.7 ± 3.5	0.29	232.3 ± 50.0	29.6 ± 3.6	0.13	2.2	43.4 ± 13.9	9.7 ± 0.8	0.22	1.3

[a] Selectivity is calculated by dividing the efficiency of dTTP (k_{pol}/K_d) by the efficiency of d4TTP or 4′-Ed4TTP.

and d4TTP. The efficiency of 4′-Ed4TMP incorporation is 0.77 μM^{-1} s^{-1}, which is about twofold less than that of dTMP incorporation but about twofold higher than that of d4TMP incorporation.

For the DNA/RNA P/T, the K_d value for dTTP by wt RT is 67.1 μM, 4.5-fold higher than that for the DNA/DNA P/T, while the k_{pol} value also increased by threefold to 65.0 s^{-1}. This result is consistent with the previously published results, indicating that polymerization usually happens faster with the DNA/RNA P/T than with the DNA/DNA P/T (7, 17, 18). The K_d value for d4TTP is 40.8 μM, slightly lower than that for dTTP, while the k_{pol} value for d4TTP is 18.4 s^{-1}, 3.5-fold less than that for dTTP, resulting in the overall efficiency of d4TMP incorporation being about 50% of that of dTMP incorporation. On the other hand, the K_d value for 4′-Ed4TTP is 11.4 μM, which is sixfold less than that for dTTP, suggesting an even tighter binding to the RT-DNA/RNA complex. In spite of the low k_{pol} value for 4′-Ed4TTP compared with that for dTTP, the overall efficiency of 4′-Ed4TMP incorporation is 1.0 μM^{-1} s^{-1}, the same as that of dTMP, and twofold higher than that of d4TMP.

Single-turnover incorporation of dTMP, d4TMP, and 4′-Ed4TMP by the RT M184V mutant. Similarly, the pre-steady-state kinetic constants for dTMP, d4TMP, and 4′-Ed4TMP incorporation by the RT M184V mutant were determined under the single-turnover conditions.

For the DNA/DNA P/T, the K_d value for dTTP with the M184V mutant is fivefold higher than that with wt RT, while the k_{pol} value with the M184V mutant is the same as that with wt RT. The K_d value for d4TTP is eightfold higher than that for dTTP, which makes the efficiency of d4TMP incorporation about sixfold less than that of dTMP incorporation. The K_d for 4′-Ed4TTP is 168.1 μM, which is only about threefold lower than that for d4TTP, and the efficiency of 4′-Ed4TMP incorporation is twofold higher than that of d4TMP incorporation but threefold lower than that of dTMP incorporation.

For the DNA/RNA P/T, the K_d for dTTP with the M184V mutant is 143.9 μM, which is twofold higher than that for the DNA/DNA P/T and also twofold higher than the K_d value for dTTP with wt RT and the DNA/RNA P/T. The K_d value for d4TTP with the M184V mutant is 232.3 μM, which is about 1.7-fold higher than that for dTTP, while the k_{pol} value for d4TTP is slightly lower than that for dTTP. For 4′-Ed4TTP, the K_d value is 43.4 μM, which is fivefold lower than that for d4TTP and threefold lower than that for dTTP. The k_{pol} value for 4′-Ed4TTP is three- to fourfold lower than that for dTTP and d4TTP. The efficiency for 4′-Ed4TMP incorporation is 0.22 μM^{-1} s^{-1}, which is twofold higher than that for d4TMP incorporation and similar to that for dTMP incorporation.

Computer modeling. The crystal structure of the HIV-1 RT-P/T-dTTP ternary complex (with DNA/DNA P/T) has revealed active-site residues that are involved in the formation of the nucleotide-binding pocket (12). With the aid of computer modeling, this structure provides a framework for predicting possible interactions of HIV-1 RT with d4TTP and 4′-Ed4TTP.

To explain the observed kinetic behaviors of 4′-Ed4TTP, we modeled an ethynyl group into the 4′ position of d4TTP according to its known geometry arranged in the crystal structure of the HIV-1 RT-DNA-dTTP ternary complex (12). We observed an additional binding of the 4′-ethynyl group at a hydrophobic pocket, which is preformed by the side chains of A114, Y115, M184, F160, and D185 (Fig. 4A). The estimated distances from the C-2 atom of the 4′-ethynyl group to Cβ of A114, to Cδ2 of F160, and to Sδ of M184 are 3.7 Å, 3.3 Å, and 3.4 Å, respectively, all of which fall into the ideal range for Van de Waals interactions.

To validate our model about the 4′-Ed4TTP binding to

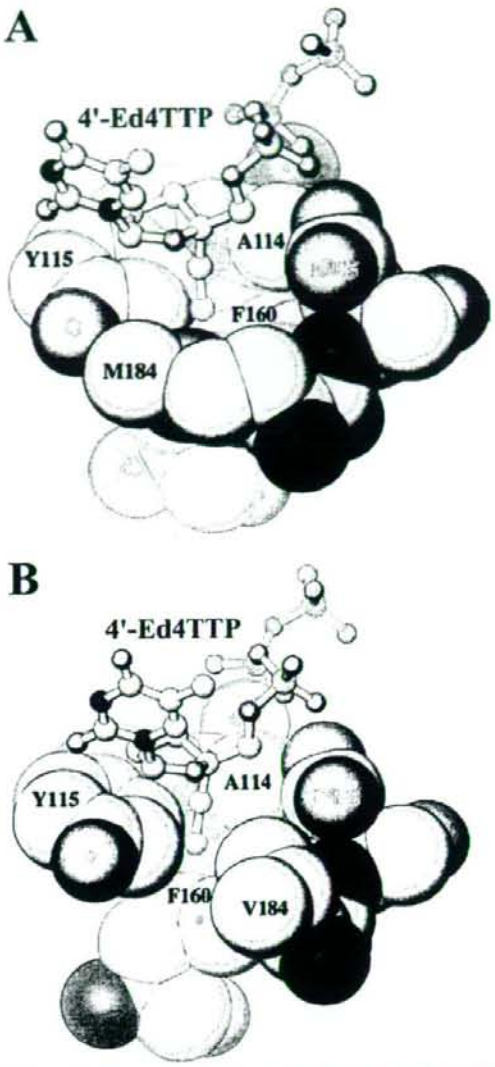

FIG. 4. Computer modeling of the 4′-Ed4TTP onto the wt RT-DNA/DNA-dTTP ternary complex (A) and the in silico mutated M184V-DNA/DNA-dTTP ternary complex (B). The modified nucleotide with the double bond formed between C-2 and C-3 was taken from the structure of d4TMP that bound to human thymidylate kinase (29) and superimposed onto the existing dNTP in the ternary complex. The ethynyl group was added using the standard ONO library database (16).

RT, we introduced mutations to the binding pocket, namely, A114M, A114L, Y115Q, F160A, F160L, M184A, M184F, and M184V. We predicted that these mutants would have lower binding affinity for 4′-Ed4TTP if the structural modifications destroy the binding pocket by filling or opening it. Unfortunately, all mutants except M184V and M184A exhibited very poor enzyme activity, making further investigation impossible.

DISCUSSION

The studies presented herein address the mechanistic basis for the inhibition of HIV-1 RT by 4′-Ed4TTP, highlighting the specific contribution from its 4′-ethynyl moiety.

4′-Ed4TTP has higher binding affinity for RT than does d4TTP. Studies with 4′-substituted 2′-deoxynucleosides have demonstrated the superior potency of the 4′-ethynyl substitution against HIV-1 (10, 19, 26, 28). Our previous steady-state study showed that 4′-Ed4TTP inhibited the DNA polymerase activity of HIV-1 RT more efficiently than did d4TTP (41). Its low steady-state K_i values imply the strong binding to HIV-1 RT (41). Here we used transient kinetic analysis to show that 4′-Ed4TTP displayed three- to fivefold-lower K_d values than its parental compound, d4TTP, in the context of both wt RT and the M184V mutant, regardless of DNA/DNA or DNA/RNA P/T. This result suggests a tighter binding of RT with 4′-Ed4TTP than with d4TTP. The efficiency of 4′-Ed4TMP incorporation (k_{pol}/K_d) is twofold higher than that of d4TMP incorporation, mostly due to the lower K_d values for 4′-Ed4TTP. Notably, 4′-Ed4TMP can be incorporated into DNA/RNA P/T by wt RT as efficiently as the natural nucleotide dTMP due to its much-reduced K_d.

The selectivity for dTTP over 4′-Ed4TTP is 0.97 with DNA/RNA P/T, twofold lower than with DNA/DNA P/T, suggesting that 4′-Ed4TTP inhibits RT more efficiently in DNA replication with RNA template than with DNA template. This is consistent with our previous steady-state measurements (41).

Incorporation of 4′-Ed4TMP by the M184V mutant. Previously using drug susceptibility assays we showed that 4′-Ed4T inhibits HIV-1 harboring the M184V mutation three to five times less efficiently than wt HIV-1 (27), a finding that is consistent with our steady-state analysis, which showed that 4′-Ed4TTP inhibits the M184V mutant two- to threefold less efficiently than wt RT (41). In the present study, we employed transient kinetic analysis to focus on drug resistance during the first turnover of DNA polymerization.

Our results showed that the efficiency of dTMP, d4TMP, and 4′-Ed4TMP incorporation by the M184V mutant RT decreased three- to sevenfold compared with wt RT. The change is mainly due to the weaker binding affinity of these nucleotides for the M184V mutant than for wt RT (Table 3). The drug-resistant M184V mutant RT has previously been subject to extensive steady-state and pre-steady-state kinetic studies. However, resulting kinetic parameters varied widely with the experimental approach, the sequence of the P/T duplex, and the nature of both the template strand and the base pairing of the incoming nucleotides (1–3, 8, 31, 39). Notably, a pre-steady-state study indicated that the overall efficiency of d4GMP incorporation by the M184V mutant was the same as the efficiency of that by wt RT, and for both wt RT and the M184V mutant, the selectivity for dGTP over d4GTP was 2 for both the DNA/DNA and DNA/RNA P/Ts (31).

The sequence of P/T used in our study came from the HIV-1 5′ untranslated region in order to mimic the initiation of viral DNA replication in vivo. We observed that the efficiency of d4TMP incorporation by the M184V mutant decreased six- and threefold for DNA/DNA and DNA/RNA P/Ts, respectively, compared with wt RT. The corresponding selectivity for dTTP over d4TTP with M184V is 6.2 and 2.2 for the two P/Ts. In comparison, the selectivity associated with wt RT in the context of DNA/DNA and DNA/RNA P/Ts is 4.5 and 2.2, respectively. The M184V mutant is not expected to exhibit drug resistance toward d4TTP or d4GTP, in agreement with the drug susceptibility studies involving d4G or d4T treatment of HIV-1 bearing the M184V mutation (27, 31).

wt RT showed a selectivity of 1.9 for dTTP over 4′-Ed4TTP with the DNA/DNA P/T and 0.97 with the DNA/RNA P/T, whereas the M184V mutant showed a selectivity of 2.8 with the DNA/DNA P/T and 1.3 with the DNA/RNA P/T, respectively. Although the M184V mutant always shows selectivity factors slightly higher than those of wt RT, the difference is not significant enough to demonstrate the resistance of the M184V mutant to 4′-Ed4TTP (Table 3). However, about threefold resistance was observed in both a steady-state kinetic study (41) and a drug susceptibility study (27). One plausible explanation for this difference is that the threefold resistance observed in the steady-state measurement was a result of amplification after multiple turnovers of enzyme reaction, which was unlikely to be detected in our pre-steady-state single-turnover experiment. A similar amplification effect was also observed in the pre-steady-state kinetic study of 3TC-TP, where the selectivity for dCTP over 3TC-TP by the M184V mutant increased by 34-fold in DNA-dependent polymerization and 140-fold in RNA-dependent polymerization compared with wt RT (8), which led to an over-1,000-fold resistance in cell culture and clinic studies (33, 34).

The structural basis for the increased binding affinity of 4′-Ed4TTP to RT compared with d4TTP. The crystal structure of the HIV-1 RT-P/T-dTTP ternary complex shows that the 3′-hydroxyl group of dTTP forms one hydrogen bond with the backbone amide of the sugar gate Y115 and another bond with the side chain of Q151 (12, 13). This structural feature suggests that in general DNA chain-terminating nucleotide analogues lacking the 3′-hydroxyl group do not bind well at the polymerase active site (12, 13) unless the loss of bonding is compensated elsewhere.

Our kinetic parameters for d4TMP incorporation are consistent with structural predictions. There are two differences between d4TTP and dTTP: (i) a double bond between C-2′–C-3′ bond and (ii) the missing 3′-hydroxyl group at C-3′ rendering d4TTP the chain terminator property. The absence of the 3′-hydroxyl group results in the loss of two hydrogen bonds as the crystal structure predicts, which accounts for the lower binding affinity for d4TTP than for dTTP as observed in our study. The contribution from the new double bond between C-2′ and C-3′ atoms is not expected to be substantial, because there is only a slight change in the sugar configuration between dTMP and d4TMP that binds to human thymidylate kinase (29). This model should predict the same kinetic behaviors not only for d4TTP and dTTP but also for other chain-terminating

nucleotide analogues and their natural parent nucleoside triphosphates, including d4GTP and dGTP. However, we are aware that d4GTP and dGTP were reported to have the same binding affinity for wt RT (31), which cannot be simply explained by our computer modeling.

Using computer modeling, we observed additional binding of the 4′-ethynyl group at a hydrophobic pocket of RT, which could increase the binding affinity of 4′-Ed4TTP for RT compared with that of d4TTP (Fig. 4A). This prediction is supported by our observation of a threefold-lower K_d value of 4′-Ed4TTP than of d4TTP (Table 3).

Consistent with our prediction that the size and shape of this pocket in the M184V mutant will be different from those in wt RT (Fig. 4B), we showed that indeed the M184V mutation had caused a 4- and 10-fold decrease in the binding affinity of 4′-Ed4TTP for RNA and DNA template, respectively.

We have also found a fivefold reduction in the binding of dTTP to the M184V mutant (Table 3). This observation is unexpected from existing crystal structures or from the above modeling, because Met184 is not in direct contact with dTTP. A possible explanation for the lower binding affinity of incoming nucleotides for the M184V mutant is that Met184 constitutes part of the nascent base-pairing pocket (12), and the M184V mutation apparently created a gap between the polymerase and the minor groove of the nascent base pair, which could indirectly affect the binding of the incoming dTTP. Similar indirect effects have been observed in RB69 DNA polymerases with the L561A and Y567A mutations (42), which are analogous to the M184V mutation in HIV-1 RT.

Inhibition of HIV-1 RT by another 4′-ethynyl-substituted nucleoside analogue, 4′-EddCTP, has been studied by Siddiqui et al. (36). The D-enantiomer of this compound strongly inhibited both wt RT and the M184V mutant. On the other hand, its L-enantiomer inhibited only wt RT, but not the M184V mutant RT. With the solved crystal structure of 4′-EddCTP, both of its D- and L-enantiomers were docked into the active site of the RT-DNA/DNA-dNTP ternary complex (36). According to the computer modeling study, the 4′-ethynyl group of both the D- and L-enantiomers was close to the Met184 residue in wt RT. In the model of the M184V mutant, the 4′-ethynyl group of the D-enantiomer showed some negative steric interaction with Val184. When the L-enantiomer was docked into the M184V mutant, there was a steric clash between the ethynyl group and Val184, which could explain the lack of inhibition of the M184V mutant by the L-enantiomer (36). Here we can make the same modeling for 4′-EddCTP as for 4′-Ed4TTP by changing the nature of the base and the enantiomer of the sugar. Our modeling also predicts that both the D- and L-enantiomers should bind wt RT, thereby terminating the replication upon incorporation of the compound. In the L-enantiomer of 4′-EddCTP, our modeling shows that the branched Val184 side chain of the M184V mutant would clash with the compound at its branching point Cγ1 or Cγ2, but this branched Val184 side chain would not clash with the D-enantiomer (Fig. 4B). Therefore, our model is consistent with the corresponding kinetic data for 4′-EddCTP.

Previously we found that 4′-Ed4TTP exhibited poor inhibitory effects on five major human DNA polymerases, α, β, γ, δ, and ε, in general (41). Particularly, we showed that human DNA polymerase β was selectively inhibited by d4TTP, but not by 4′-Ed4TTP (with a more-than-100-fold difference in 50% inhibitory concentration) (41). Because the crystal structures of polymerase β are available (32), we could extend computer modeling techniques to this polymerase. By adopting modeling approaches similar to what we have done for HIV-1 RT, we found that the 4′-ethynyl group of 4′-Ed4TTP could not fit into the ternary complex due to a steric clash with the F272 side chain, which could explain its apparent lower toxicity in the cell (data not shown).

In conclusion, our pre-steady-state kinetic study together with computer modeling illustrated the fact that 4′-Ed4TTP is a better RT inhibitor than d4TTP due to the additional binding of the 4′-ethynyl group at a preformed hydrophobic pocket in the RT active site. Inhibition of RT was greater in cells treated with 4′-Ed4T than in those treated with d4T, and 4′-Ed4T treatment showed a unique resistance profile (27), much less cytotoxicity (6), and superior persistence of antiviral activity (30). All these features make 4′-Ed4T a promising candidate for HIV-1 chemotherapy.

ACKNOWLEDGMENTS

We thank William Konigsberg for the access to the KinTek Rapid Quench apparatus in his laboratory and carefully reading the manuscript. We thank Stephen Hughes for providing us with the wt RT plasmid.

This work was supported by Public Health Service grant AI-38204 from the National Institutes of Health to Y.-C.C. Y.-C.C. is a fellow of the National Foundation for Cancer Research.

REFERENCES

1. **Back, N. K., M. Nijhuis, W. Keulen, C. A. Boucher, B. O. Oude Essink, A. B. van Kuilenburg, A. H. van Gennip, and B. Berkhout.** 1996. Reduced replication of 3TC-resistant HIV-1 variants in primary cells due to a processivity defect of the reverse transcriptase enzyme. EMBO J. **15**:4040–4049.
2. **Boyer, P. L., and S. H. Hughes.** 1995. Analysis of mutations at position 184 in reverse transcriptase of human immunodeficiency virus type 1. Antimicrob. Agents Chemother. **39**:1624–1628.
3. **Chao, S. F., V. L. Chan, P. Juranka, A. H. Kaplan, R. Swanstrom, and C. A. Hutchison III.** 1995. Mutational sensitivity patterns define critical residues in the palm subdomain of the reverse transcriptase of human immunodeficiency virus type 1. Nucleic Acids Res. **23**:803–810.
4. **Chen, C. H., and Y. C. Cheng.** 1989. Delayed cytotoxicity and selective loss of mitochondrial DNA in cells treated with the anti-human immunodeficiency virus compound 2′,3′-dideoxycytidine. J. Biol. Chem. **264**:11934–11937.
5. **Chen, C. H., M. Vazquez-Padua, and Y. C. Cheng.** 1991. Effect of anti-human immunodeficiency virus nucleoside analogs on mitochondrial DNA and its implication for delayed toxicity. Mol. Pharmacol. **39**:625–628.
6. **Dutschman, G. E., S. P. Grill, E. A. Gullen, K. Haraguchi, S. Takeda, H. Tanaka, M. Baba, and Y. C. Cheng.** 2004. Novel 4′-substituted stavudine analog with improved anti-human immunodeficiency virus activity and decreased cytotoxicity. Antimicrob. Agents Chemother. **48**:1640–1646.
7. **Feng, J. Y., and K. S. Anderson.** 1999. Mechanistic studies comparing the incorporation of (+) and (−) isomers of 3TCTP by HIV-1 reverse transcriptase. Biochemistry **38**:55–63.
8. **Feng, J. Y., and K. S. Anderson.** 1999. Mechanistic studies examining the efficiency and fidelity of DNA synthesis by the 3TC-resistant mutant (184V) of HIV-1 reverse transcriptase. Biochemistry **38**:9440–9448.
9. **Hamamoto, Y., H. Nakashima, T. Matsui, A. Matsuda, T. Ueda, and N. Yamamoto.** 1987. Inhibitory effect of 2′,3′-didehydro-2′,3′-dideoxynucleosides on infectivity, cytopathic effects, and replication of human immunodeficiency virus. Antimicrob. Agents Chemother. **31**:907–910.
10. **Haraguchi, K., S. Takeda, H. Tanaka, T. Nitanda, M. Baba, G. E. Dutschman, and Y. C. Cheng.** 2003. Synthesis of a highly active new anti-HIV agent 2′,3′-didehydro-3′-deoxy-4′-ethynylthymidine. Bioorg. Med. Chem. Lett. **13**:3775–3777.
11. **Hsu, C. H., R. Hu, G. E. Dutschman, G. Yang, P. Krishnan, H. Tanaka, M. Baba, and Y. C. Cheng.** 2007. Comparison of the phosphorylation of 4′-ethynyl 2′,3′-dihydro-3′-deoxythymidine with that of other anti-human immunodeficiency virus thymidine analogs. Antimicrob. Agents Chemother. **51**:1687–1693.
12. **Huang, H., R. Chopra, G. L. Verdine, and S. C. Harrison.** 1998. Structure of a covalently trapped catalytic complex of HIV-1 reverse transcriptase: implications for drug resistance. Science **282**:1669–1675.

13. **Jamburuthugoda, V. K., D. Guo, J. E. Wedekind, and B. Kim.** 2005. Kinetic evidence for interaction of human immunodeficiency virus type 1 reverse transcriptase with the 3′-OH of the incoming dTTP substrate. Biochemistry **44:**10635–10643.
14. **Johnson, K. A.** 1993. Conformational coupling in DNA polymerase fidelity. Annu. Rev. Biochem. **62:**685–713.
15. **Johnson, K. J., J. Varani, and J. E. Smolen.** 1992. Neutrophil activation and function in health and disease. Immunol. Ser. **57:**1–46.
16. **Jones, T. A., J. Y. Zou, S. W. Cowan, and M. Kjeldgaard.** 1991. Improved methods for building protein models in electron density maps and the location of errors in these models. Acta Crystallogr. A **47:**110–119.
17. **Kati, W. M., K. A. Johnson, L. F. Jerva, and K. S. Anderson.** 1992. Mechanism and fidelity of HIV reverse transcriptase. J. Biol. Chem. **267:**25988–25997.
18. **Kerr, S. G., and K. S. Anderson.** 1997. Pre-steady-state kinetic characterization of wild type and 3′-azido-3′-deoxythymidine (AZT) resistant human immunodeficiency virus type 1 reverse transcriptase: implication of RNA directed DNA polymerization in the mechanism of AZT resistance. Biochemistry **36:**14064–14070.
19. **Kodama, E. I., S. Kohgo, K. Kitano, H. Machida, H. Gatanaga, S. Shigeta, M. Matsuoka, H. Ohrui, and H. Mitsuya.** 2001. 4′-Ethynyl nucleoside analogs: potent inhibitors of multidrug-resistant human immunodeficiency virus variants in vitro. Antimicrob. Agents Chemother. **45:**1539–1546.
20. **Krishnan, P., J. Y. Liou, and Y. C. Cheng.** 2002. Phosphorylation of pyrimidine L-deoxynucleoside analog diphosphates. Kinetics of phosphorylation and dephosphorylation of nucleoside analog diphosphates and triphosphates by 3-phosphoglycerate kinase. J. Biol. Chem. **277:**31593–31600.
21. **Lin, T. S., R. F. Schinazi, M. S. Chen, E. Kinney-Thomas, and W. H. Prusoff.** 1987. Antiviral activity of 2′,3′-dideoxycytidin-2′-ene (2′,3′-dideoxy-2′,3′-didehydrocytidine) against human immunodeficiency virus in vitro. Biochem. Pharmacol. **36:**311–316.
22. **Lin, T. S., R. F. Schinazi, and W. H. Prusoff.** 1987. Potent and selective in vitro activity of 3′-deoxythymidin-2′-ene (3′-deoxy-2′,3′-didehydrothymidine) against human immunodeficiency virus. Biochem. Pharmacol. **36:**2713–2718.
23. **Medina, D. J., C. H. Tsai, G. D. Hsiung, and Y. C. Cheng.** 1994. Comparison of mitochondrial morphology, mitochondrial DNA content, and cell viability in cultured cells treated with three anti-human immunodeficiency virus dideoxynucleosides. Antimicrob. Agents Chemother. **38:**1824–1828.
24. **Mitsuya, H., R. Yarchoan, and S. Broder.** 1990. Molecular targets for AIDS therapy. Science **249:**1533–1544.
25. **Murakami, E., A. S. Ray, R. F. Schinazi, and K. S. Anderson.** 2004. Investigating the effects of stereochemistry on incorporation and removal of 5-fluorocytidine analogs by mitochondrial DNA polymerase gamma: comparison of D- and L-D4FC-TP. Antivir. Res. **62:**57–64.
26. **Nakata, H., M. Amano, Y. Koh, E. Kodama, G. Yang, C. M. Bailey, S. Kohgo, H. Hayakawa, M. Matsuoka, K. S. Anderson, Y. C. Cheng, and H. Mitsuya.** 2007. Activity against human immunodeficiency virus type 1, intracellular metabolism, and effects on human DNA polymerases of 4′-ethynyl-2-fluoro-2′-deoxyadenosine. Antimicrob. Agents Chemother. **51:**2701–2708.
27. **Nitanda, T., X. Wang, H. Kumamoto, K. Haraguchi, H. Tanaka, Y. C. Cheng, and M. Baba.** 2005. Anti-human immunodeficiency virus type 1 activity and resistance profile of 2′,3′-didehydro-3′-deoxy-4′-ethynylthymidine in vitro. Antimicrob. Agents Chemother. **49:**3355–3360.
28. **Ohrui, H., S. Kohgo, K. Kitano, S. Sakata, E. Kodama, K. Yoshimura, M. Matsuoka, S. Shigeta, and H. Mitsuya.** 2000. Syntheses of 4′-C-ethynyl-beta-D-arabino- and 4′-C-ethynyl-2′-deoxy-beta-D-ribo-pentofuranosylpyrimidines and -purines and evaluation of their anti-HIV activity. J. Med. Chem. **43:**4516–4525.
29. **Ostermann, N., D. Segura-Pena, C. Meier, T. Veit, C. Monnerjahn, M. Konrad, and A. Lavie.** 2003. Structures of human thymidylate kinase in complex with prodrugs: implications for the structure-based design of novel compounds. Biochemistry **42:**2568–2577.
30. **Paintsil, E., G. E. Dutschman, R. Hu, S. P. Grill, W. Lam, M. Baba, H. Tanaka, and Y. C. Cheng.** 2007. Intracellular metabolism and persistence of the anti-human immunodeficiency virus activity of 2′,3′-didehydro-3′-deoxy-4′-ethynylthymidine, a novel thymidine analog. Antimicrob. Agents Chemother. **51:**3870–3879.
31. **Ray, A. S., Z. Yang, J. Shi, A. Hobbs, R. F. Schinazi, C. K. Chu, and K. S. Anderson.** 2002. Insights into the molecular mechanism of inhibition and drug resistance for HIV-1 RT with carbovir triphosphate. Biochemistry **41:**5150–5162.
32. **Sawaya, M. R., R. Prasad, S. H. Wilson, J. Kraut, and H. Pelletier.** 1997. Crystal structures of human DNA polymerase beta complexed with gapped and nicked DNA: evidence for an induced fit mechanism. Biochemistry **36:**11205–11215.
33. **Schinazi, R. F., R. M. Lloyd, Jr., M. H. Nguyen, D. L. Cannon, A. McMillan, N. Ilksoy, C. K. Chu, D. C. Liotta, H. Z. Bazmi, and J. W. Mellors.** 1993. Characterization of human immunodeficiency viruses resistant to oxathiolane-cytosine nucleosides. Antimicrob. Agents Chemother. **37:**875–881.
34. **Schuurman, R., M. Nijhuis, R. van Leeuwen, P. Schipper, D. de Jong, P. Collis, S. A. Danner, J. Mulder, C. Loveday, C. Christopherson, et al.** 1995. Rapid changes in human immunodeficiency virus type 1 RNA load and appearance of drug-resistant virus populations in persons treated with lamivudine (3TC). J. Infect. Dis. **171:**1411–1419.
35. **Selmi, B., J. Boretto, J. M. Navarro, J. Sire, S. Longhi, C. Guerreiro, L. Mulard, S. Sarfati, and B. Canard.** 2001. The valine-to-threonine 75 substitution in human immunodeficiency virus type 1 reverse transcriptase and its relation with stavudine resistance. J. Biol. Chem. **276:**13965–13974.
36. **Siddiqui, M. A., S. H. Hughes, P. L. Boyer, H. Mitsuya, Q. N. Van, C. George, S. G. Sarafinanos, and V. E. Marquez.** 2004. A 4′-C-ethynyl-2′,3′-dideoxynucleoside analogue highlights the role of the 3′-OH in anti-HIV active 4′-C-ethynyl-2′-deoxy nucleosides. J. Med. Chem. **47:**5041–5048.
37. **Thrall, S. H., R. Krebs, B. M. Wohrl, L. Cellai, R. S. Goody, and T. Restle.** 1998. Pre-steady-state kinetic characterization of RNA-primed initiation of transcription by HIV-1 reverse transcriptase and analysis of the transition to a processive DNA-primed polymerization mode. Biochemistry **37:**13349–13358.
38. **Vaccaro, J. A., K. M. Parnell, S. A. Terezakis, and K. S. Anderson.** 2000. Mechanism of inhibition of the human immunodeficiency virus type 1 reverse transcriptase by d4TTP: an equivalent incorporation efficiency relative to the natural substrate dTTP. Antimicrob. Agents Chemother. **44:**217–221.
39. **Wakefield, J. K., S. A. Jablonski, and C. D. Morrow.** 1992. In vitro enzymatic activity of human immunodeficiency virus type 1 reverse transcriptase mutants in the highly conserved YMDD amino acid motif correlates with the infectious potential of the proviral genome. J. Virol. **66:**6806–6812.
40. **Wohrl, B. M., R. Krebs, R. S. Goody, and T. Restle.** 1999. Refined model for primer/template binding by HIV-1 reverse transcriptase: pre-steady-state kinetic analyses of primer/template binding and nucleotide incorporation events distinguish between different binding modes depending on the nature of the nucleic acid substrate. J. Mol. Biol. **292:**333–344.
41. **Yang, G., G. E. Dutschman, C. J. Wang, H. Tanaka, M. Baba, K. S. Anderson, and Y. C. Cheng.** 2007. Highly selective action of triphosphate metabolite of 4′-ethynyl D4T: a novel anti-HIV compound against HIV-1 RT. Antivir. Res. **73:**185–191.
42. **Zhang, H., C. Rhee, A. Bebenek, J. W. Drake, J. Wang, and W. Konigsberg.** 2006. The L561A substitution in the nascent base-pair binding pocket of RB69 DNA polymerase reduces base discrimination. Biochemistry **45:**2211–2220.

JOURNAL OF VIROLOGY, Jan. 2008, p. 588–592 Vol. 82, No. 1
0022-538X/08/$08.00+0 doi:10.1128/JVI.01697-07

Heptad Repeat-Derived Peptides Block Protease-Mediated Direct Entry from the Cell Surface of Severe Acute Respiratory Syndrome Coronavirus but Not Entry via the Endosomal Pathway▽

Makoto Ujike,[1]† Hiroki Nishikawa,[2]† Akira Otaka,[3] Naoki Yamamoto,[4] Norio Yamamoto,[4] Masao Matsuoka,[5] Eiichi Kodama,[5] Nobutaka Fujii,[2,5]* and Fumihiro Taguchi[1]*

Department of Virology III, National Institute of Infectious Disease, Gakuen 4-7-1, Musashi-murayama, Tokyo 208-0011, Japan[1]; Graduate School of Pharmaceutical Sciences, Kyoto University, Sakyo-ku, Kyoto 606-8501, Japan[2]; Graduate School of Pharmaceutical Sciences, The University of Tokushima, Tokushima 770-8505, Japan[3]; Department of Molecular Virology, Tokyo Medical and Dental University, 1-5-45 Yushima, Bunkyo-ku, Tokyo 113-8519, Japan[4]; and Institute for Virus Research, Kyoto University, Sakyo-ku, Kyoto 606-8507, Japan[5]

Received 6 August 2007/Accepted 6 October 2007

The peptides derived from the heptad repeat (HRP) of severe acute respiratory syndrome coronavirus (SCoV) spike protein (sHRPs) are known to inhibit SCoV infection, yet their efficacies are fairly low. Recently our research showed that some proteases facilitated SCoV's direct entry from the cell surface, resulting in a more efficient infection than the previously known infection via endosomal entry. To compare the inhibitory effect of the sHRP in each pathway, we selected two sHRPs, which showed a strong inhibitory effect on the interaction of two heptad repeats in a rapid and virus-free in vitro assay system. We found that they efficiently inhibited SCoV infection of the protease-mediated cell surface pathway but had little effect on the endosomal pathway. This finding suggests that sHRPs may effectively prevent infection in the lungs, where SCoV infection could be enhanced by proteases produced in this organ. This is the first observation that HRP exhibits different effects on virus that takes the endosomal pathway and virus that enters directly from the cell surface.

Severe acute respiratory syndrome (SARS) coronavirus (SCoV) is a causative agent of life-threatening SARS (4, 7, 15, 31). Although the first outbreak of SARS was stamped out, an effective antiviral drug is still required for the treatment and prevention of possible future outbreaks. SCoV is an enveloped virus and enters cells via fusion between the cellular membrane and its envelope. SCoV membrane fusion is mediated by the spike (S) protein, which is classified as a class I fusion protein. One of the most important features of class I fusion proteins is the conserved heptad repeat regions (HR1 and HR2) which play an essential role in virus-cell fusion activities (3, 6, 10, 28). In the fusion process, HR1 forms an interior, trimeric coiled-coil structure to which HR2 binds in an antiparallel fashion, resulting in the formation of a six-helix bundle. This structure brings viral and cellular membranes into close proximity to facilitate membrane fusion. Synthetic short peptides derived from the HR (HRP) of class I fusion proteins have been shown to block the interaction of HR1-HR2 complexes, resulting in the inhibition of a number of viral infections, including those of retroviruses (11, 14, 21, 23, 32, 38, 39), paramyxoviruses (12, 16, 30, 36, 42–44), filovirus (37), and coronavirus (2). Similarly, HRP of SCoV S (sHRP) could also inhibit SCoV and human immunodeficiency virus (HIV)/SCoV-pseudotyped virus infection (1, 18, 24, 45). However, these inhibitory effects were significantly less than those of one of the most effective HRPs from HIV type 1 (HIV-1) (39) and even those from the same family, murine coronavirus mouse hepatitis virus (MHV) (2).

The major organs targeted by SCoV are the lungs and intestines, although the virus grows in a variety of tissues that express angiotensin-converting enzyme 2 (ACE2). Recently we and others showed that SCoV uses two distinct entry pathways depending on the presence of proteases (20, 33, 34). In the absence of proteases, SCoV enters the cell via an endosomal pathway (9, 26, 41), with the S protein activated for fusion by the cathepsin L protease, which is active only under acidic conditions in the endosome (8, 33). In contrast, in the presence of protease, SCoV virion S proteins attach to ACE2 on the host cell surface and are activated for fusion by proteases such as trypsin or elastase, which leads to envelope-plasma membrane fusion and direct entry from the cell surface (20, 33, 34). Infection via the cell surface is more than 100 times more efficient than infection via the endosomal pathway (20). These results suggested the possibility that the severe illnesses in the lung and intestine could be due to the enhancement of direct SCoV cell surface entry mediated by proteases produced in these organs (20).

Although previous studies have described the inhibitory effects of the sHRP on SCoV infection via the endosomal path-

* Corresponding author. Mailing address for F. Taguchi: Department of Virology III, National Institute of Infectious Disease, Gakuen 4-7-1, Musashi-murayama, Tokyo 208-0011, Japan. Phone: 81-42-561-0771, ext. 533. Fax: 81-42-567-5631. E-mail: ftaguchi@nih.go.jp. Mailing address for N. Fujii: Graduate School of Pharmaceutical Sciences, Kyoto University, Sakyo-ku, Kyoto 606-8501, Japan. Phone: 81-75-753-4511. Fax: 81-75-753-4570. E-mail: nfujii@pharm.kyoto-u.ac.jp.
† M.U. and H.N. contributed equally to this work.
▽ Published ahead of print on 17 October 2007.

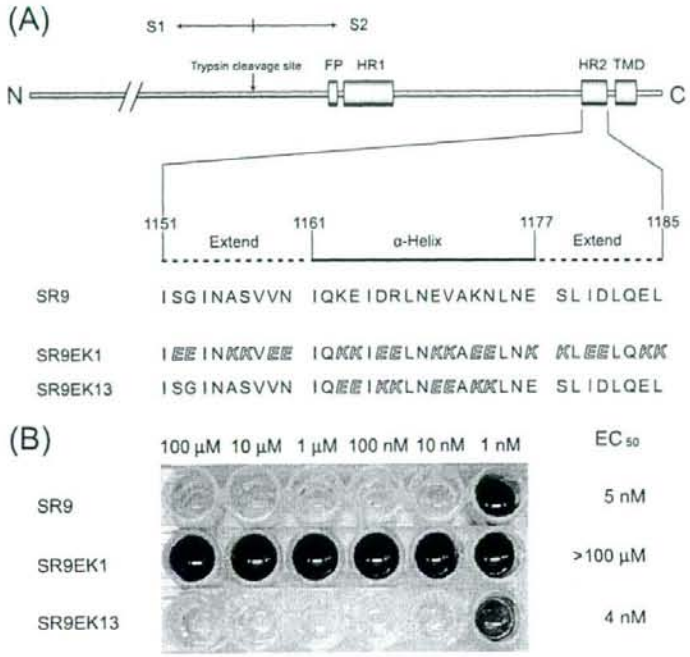

FIG. 1. (A) Schematic of SCoV S protein and sequences of native sHRP (SR9) and its EK substitution derivatives. The S protein contains two α-helical heptad repeats (HR1 and HR2), a putative fusion peptide (FP), a transmembrane domain (TMD), and a trypsin cleavage site (17). The expanded region shows the amino acid sequence of HR2 (SR9), which consists of two extended parts (1151 to 1160 and 1178 to 1185) and one α-helix part (1161 to 1177). Substituted EKs are shown with italic white letters. (B) In vitro binding inhibition assay of HRPs. GST-HR2-coated plates were incubated with MBP-HR1 in the presence of various concentrations (1 nM to 100 μM) of sHRP. Inhibitory potency of the peptide was assessed using the anti-MBP antibody-alkaline phosphatase conjugate and staining with 5-bromo-4-chloro-3-indolylphosphate.

way (1, 18, 24, 45), little is known about their effects on the protease-mediated cell surface pathway. Thus, in this study, we reevaluated the inhibitory effects of the sHRP on infection via the two distinct pathways of SCoV entry.

Recent studies of the X-ray crystal structure of the SCoV S HR1-HR2 complex have shown that the HR2 peptide consists of two extended regions and one α-helical region (35, 40). Since we have found that HRPs with replacement by the X-EE-XX-KK sequence in the HIV-1 HR2 region exhibited potent anti-HIV-1 activity (27), we chose to modify the α-helical region of HRP derived from SCoV S HR2 (sHRP) and also to prepare the control peptide SR9EK1 without sequence relatedness (Fig. 1A). To estimate these sHRPs, we established a rapid and virus-free in vitro novel assay system based on the inhibition of HR1-HR2 complex formation. Two fusion proteins (maltose binding protein [MBP]-HR1 [amino acid residues of the S protein, 892 to 964] and glutathione *S*-transferase [GST]-HR2 [1141 to 1192]) were expressed using *Escherichia coli* and purified using amylose resin (New England Biolabs) and glutathione Sepharose 4B (GE Healthcare, Bucks, United Kingdom), respectively. An enzyme-linked immunosorbent assay plate was coated with GST-HR2 dissolved in sodium carbonate buffer (pH 8.5), 3.6 μg/ml in concentration, by incubation at 4°C for 8 h. After bovine serum albumin blocking (1 mg/ml) at 4°C for 2.5 h, GST-HR2 on the plate was allowed to bind the MBP-HR1 protein (8.8 μg/ml) by incubation at 37°C for 1.5 h in the presence of various concentrations of sHRPs to be examined for inhibition activity. After the plate was washed, the inhibiting potency of the peptide was assessed by colorimetric analyses using the anti-MBP antibody-alkaline phosphatase conjugate (Sigma) with a 1:1,000 dilution with incubation at 4°C for 1 h and then staining with BluePhos microwell phosphatase (KPL). As shown in Fig. 1B, SR9 and SR9EK13 showed significant binding inhibition in a nanomolar range, whereas the control, SR9EK1, without sequence relatedness, had no inhibitory effect at a concentration of 100 μM.

We tested the inhibitory effects of SR9 and SR9EK13 on SCoV entry, since these sHRPs were found to have a strong binding inhibition activity, along with the control peptide SR9EK1. We examined their effects on both the endosomal and protease-mediated cell surface entry processes. Viral entry via the endosome was examined as described previously with a slight modification (20). In brief, VeroE6 cells were pretreated with each sHRP at 37°C for 30 min and then inoculated with SCoV (multiplicity of infection = 1.0) and incubated on ice for 30 min to allow viral attachment to ACE2 but not viral entry. After removal of unattached viruses, the cells were incubated at 37°C for 6 h. Viral entry was measured by quantifying the newly synthesized mRNA9 using real-time PCR (20). To evaluate entry via the cell surface, the cells were pretreated with 1

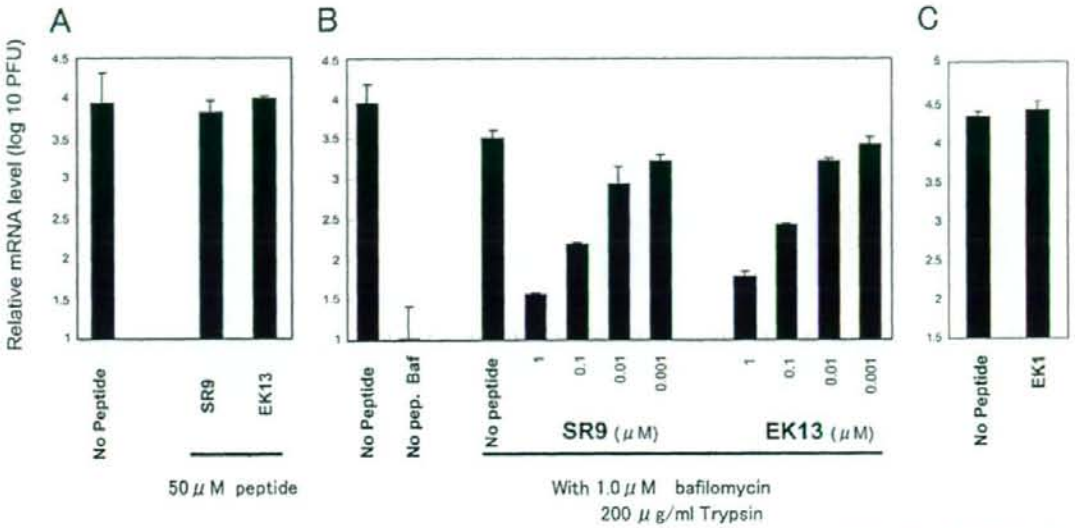

FIG. 2. Inhibitory effect of sHRPs on SCoV infections via the endosomal pathway (A) or protease-mediated cell-surface pathway (B). (A) VeroE6 cells were pretreated with 50 μM sHRPs at 37°C for 30 min, placed on ice for 10 min, and then inoculated with SCoV at a multiplicity of infection of 1.0 on ice for 30 min. After the removal of unbound virus, the cells were incubated in medium containing 50 μM sHRPs at 37°C for 6 h. (B) Cells pretreated with 1 μM Baf and sHRPs at the indicated concentrations were inoculated with SCoV as described above. After the removal of unbound virus, the cells were treated with 200 μg/ml L-1-tosylamide-2-phenylethyl chloromethyl ketone-treated trypsin at room temperature for 5 min and incubated at 37°C for 6 h. sHRP and Baf were present in the media in all steps at indicated concentrations. To measure amounts of viruses that entered cells, cells were infected with 10-fold-stepwise-diluted SARS-CoV from 10^6 to 10^2 PFU without Baf and trypsin and the amounts of mRNA9 were quantified by real-time PCR. Amounts of viral entry in this study were calculated from a calibration line obtained as described above and are shown as relative mRNA levels (20). (C) EK1 has no sequential similarity to sHRP and showed no inhibitory effect in vitro. Cells were treated with 1 μM EK1 as a control peptide, and other procedures were performed as described for panel B.

μM bafilomycin (Baf), which blocks SCoV endosomal entry, at 37°C for 30 min before SCoV inoculation. After removal of unattached viruses, the cells were treated with trypsin (0.2 mg/ml) for 5 min at room temperature and viral entry was measured as described above. Each sHRP and/or Baf was present in the media in all steps at various concentrations. In the absence of proteases, these sHRPs showed no measurable inhibitory effect on SCoV endosomal infection even at concentrations as high as 50 μM, despite showing a potent inhibitory effect in vitro (Fig. 2A). This lack of inhibition is consistent with previous observations that the same or homologous-sequence sHRPs had no inhibitory effect on SCoV infection at high concentrations of 10 μM (45) or 50 μM (1), respectively. In contrast, when SCoV was allowed to enter cells via the cell surface by treatment with protease and Baf, these sHRPs showed a strong inhibitory effect on SCoV infection in a dose-dependent manner (Fig. 2B). At a concentration of 0.1 μM, the SR9 sHRP reduced newly synthesized mRNA9 levels by about 10-fold, while an sHRP concentration of 1 μM saw a 50-fold decrease. The control sHRP, SR9EK1, did not inhibit SCoV cell-surface-mediated infection even at the concentration of 1 μM, indicating that the inhibition is peptide sequence specific (Fig. 2C). We finally evaluated the inhibitory effect of sHRPs in the presence of trypsin but without Baf treatment. These conditions may resemble the situation of patients with severe SARS, in which some proteases were produced in the infected lung and intestinal tissue. Under these conditions, these sHRPs also showed a potent inhibitory effect on SCoV infection (Fig. 3).

The present study indicates that our sHRPs fail to inhibit endosome-mediated SCoV infection. This finding is consistent with those of previous studies indicating that sHRPs have a low inhibitory effect on endosomal infection of native SCoV. The reported 50% effective dose (EC_{50}) was 3.68 to 19.0 μM (1, 18, 45). However, our results suggest that sHRPs, which showed no measurable inhibitory effect on SCoV endosomal infection, have a very strong inhibitory effect on protease-mediated cell surface SCoV infection; the EC_{50} was less than 100 nM (Fig. 2B and 3). Cell surface infection of SCoV is anticipated to occur in the lungs of SARS patients, since various types of inflammatory cells infiltrate the lung of the patients (25), and thus elastase, a protease produced in lung inflammation (13) and shown to enhance SCoV infection in cultured cells (20), could enhance SCoV infection in the lung by facilitating the infection from cell surface. Inhibitory effects of sHRPs on cell surface infection may help prevent severe damage by SCoV infection in the major target organ. Thus, the sHRPs shown in this study would be effective anti-SARS therapeutic drugs.

A few possibilities are conceivable for the explanation of an inefficient inhibitory effect of sHRPs in infection via the endosomal pathway. One is the failure of sHRPs to be trafficked to the endosome vehicles from culture medium. Thus, their concentration in the endosome is not sufficient to prevent SCoV infection. Alternatively, sHRPs may be sufficiently transported

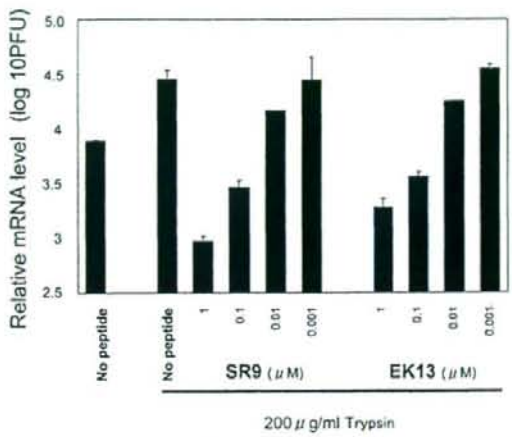

FIG. 3. Effective inhibition by HRPs of SCoV infection in the presence of exogenous trypsin. VeroE6 cells pretreated with sHRPs at the indicated concentrations were inoculated with SCoV as described in the legend to Fig. 2. After the removal of unbound virus, the cells were treated with 200 μg/ml L-1-tosylamide-2-phenylethyl chloromethyl ketone-treated trypsin at room temperature for 5 min and incubated at 37°C for 6 h. sHRPs were present in the media in all steps at the indicated concentrations. The relative viral mRNA9 was measured quantitatively by real-time PCR as described in the legend to Fig. 2. In this assay, cells were not treated with Baf throughout the experiment.

to the endosome but are inactivated by the low-pH environment or are degraded or digested with proteases present in the endosome. Another possibility is that the conformation of the cleaved S protein in the acidic environment of the endosome is different from that in a neutral pH and the sHRP fails to bind to the S protein in the former environment even if six-helix bundles with intramolecular HR2 are formed under both conditions. We are currently studying whether the inefficient inhibition of virus entry into cells could be attributed to one of those possibilities, or even another.

Interestingly, the EC_{50} (approximately 680 μM) of HRP of Ebola virus (37), which is thought to enter cells via an endosomal pathway, is remarkably higher than those of other viruses which enter cells directly from the cell surface. The inhibition with HRP of influenza virus infection, which also uses an endosomal pathway, has not yet been reported, even though its hemagglutinin protein is the prototype class I fusion protein and its cell entry mechanism has been extensively studied. In contrast, HRP of avian leucosis sarcoma virus, which uses the endosomal pathway, was reported to inhibit the infection fairly efficiently (EC_{50} = 25 to 170 nM) (5, 23). The inhibition, however, was executed during the conformational rearrangement of the envelope protein that occurs on the cell surface following attachment to the receptor and facilitates the exposure of HRs but not later than the transport into the endosome, where the avian leucosis sarcoma virus genome enters the cytoplasm by its envelope and endosomal membrane fusion in a low-pH environment (19, 22, 23). These observations together with those of the present study and others (1, 18, 24, 45) suggest that the HRPs have very low or little inhibitory effect in the endosome. If the above assumption is correct and the HRPs were designed to be efficiently transferred into the endosome and to be stable in the environment, they may be new antiviral candidates against those viruses that take the endosomal entry pathway, such as influenza virus, Ebola virus, and SCoV. Thus, detailed molecular studies on SCoV and the sHRP will provide a good model for the development and evaluation of such endosome-philic antiviral peptide inhibitors.

Recent studies have reported that the low inhibitory effect of the SCoV sHRP compared to that of the MHV HRP could be attributed to the weaker interaction of the SCoV S HR1-HR2 complex versus that of MHV S (1, 2). However, SCoV infection was efficiently blocked by sHRP under certain conditions, as revealed in this study; the concentration of sHRPs needed to inhibit SCoV infection is even lower than that required for MHV inhibition (1, 2). The apparent difference between MHV and SCoV infection is the pathway used to enter cells; the former enters directly from the cell surface, whereas the latter takes an endosomal pathway. Both MHV and SCoV infections were efficiently blocked when these viruses utilized the cell surface pathway for entry. These observations suggest that the lower HRP inhibitory effect on SCoV could be due to different entry pathways between SCoV and MHV rather than the weaker interaction of the HRP and SCoV S. To further explore this possibility, studies are ongoing to determine the effect of MHV sHRPs on infection by MHV-2, which, like SCoV, utilizes an endosomal infection pathway (29).

We thank Miyuki Kawase for her excellent technical assistance and Shutoku Matsuyama for his valuable discussions.

This work was financially supported by grants from the Ministry of Education, Culture, Sports, Science and Technology.

REFERENCES

1. **Bosch, B. J., B. E. Martina, R. Van Der Zee, J. Lepault, B. J. Haijema, C. Versluis, A. J. Heck, R. De Groot, A. D. Osterhaus, and P. J. Rottier.** 2004. Severe acute respiratory syndrome coronavirus (SARS-CoV) infection inhibition using spike protein heptad repeat-derived peptides. Proc. Natl. Acad. Sci. USA **101**:8455–8460.
2. **Bosch, B. J., R. van der Zee, C. A. de Haan, and P. J. Rottier.** 2003. The coronavirus spike protein is a class I virus fusion protein: structural and functional characterization of the fusion core complex. J. Virol. **77**:8801–8811.
3. **Chan, W. E., C. K. Chuang, S. H. Yeh, M. S. Chang, and S. S. Chen.** 2006. Functional characterization of heptad repeat 1 and 2 mutants of the spike protein of severe acute respiratory syndrome coronavirus. J. Virol. **80**:3225–3237.
4. **Drosten, C., S. Gunther, W. Preiser, S. van der Werf, H. R. Brodt, S. Becker, H. Rabenau, M. Panning, L. Kolesnikova, R. A. Fouchier, A. Berger, A. M. Burguiere, J. Cinatl, M. Eickmann, N. Escriou, K. Grywna, S. Kramme, J. C. Manuguerra, S. Muller, V. Rickerts, M. Sturmer, S. Vieth, H. D. Klenk, A. D. Osterhaus, H. Schmitz, and H. W. Doerr.** 2003. Identification of a novel coronavirus in patients with severe acute respiratory syndrome. N. Engl. J. Med. **348**:1967–1976.
5. **Earp, L. J., S. E. Delos, R. C. Netter, P. Bates, and J. M. White.** 2003. The avian retrovirus avian sarcoma/leukosis virus subtype A reaches the lipid mixing stage of fusion at neutral pH. J. Virol. **67**:3058–3066.
6. **Follis, K. E., J. York, and J. H. Nunberg.** 2005. Serine-scanning mutagenesis studies of the C-terminal heptad repeats in the SARS coronavirus S glycoprotein highlight the important role of the short helical region. Virology **341**:122–129.
7. **Fouchier, R. A., T. Kuiken, M. Schutten, G. van Amerongen, G. J. van Doornum, B. G. van den Hoogen, M. Peiris, W. Lim, K. Stohr, and A. D. Osterhaus.** 2003. Aetiology: Koch's postulates fulfilled for SARS virus. Nature **423**:240.
8. **Huang, I. C., B. J. Bosch, F. Li, W. Li, K. H. Lee, S. Ghiran, N. Vasilieva, T. S. Dermody, S. C. Harrison, P. R. Dormitzer, M. Farzan, P. J. Rottier, and H. Choe.** 2006. SARS coronavirus, but not human coronavirus NL63, utilizes cathepsin L to infect ACE2-expressing cells. J. Biol. Chem. **281**:3198–3203.
9. **Inoue, Y., N. Tanaka, Y. Tanaka, S. Inoue, K. Morita, M. Zhuang, T. Hattori, and K. Sugamura.** 2007. Clathrin-dependent entry of severe acute respira-

tory syndrome coronavirus into target cells expressing ACE2 with the cytoplasmic tail deleted. J. Virol. 81:8722–8729.
10. Jahn, R., T. Lang, and T. C. Sudhof. 2003. Membrane fusion. Cell 112:519–533.
11. Jiang, S., K. Lin, N. Strick, and A. R. Neurath. 1993. HIV-1 inhibition by a peptide. Nature 365:113.
12. Joshi, S. B., R. E. Dutch, and R. A. Lamb. 1998. A core trimer of the paramyxovirus fusion protein: parallels to influenza virus hemagglutinin and HIV-1 gp41. Virology 248:20–34.
13. Kawabata, K., T. Hagio, and S. Matsuoka. 2002. The role of neutrophil elastase in acute lung injury. Eur. J. Pharmacol. 451:1–10.
14. Kilby, J. M., S. Hopkins, T. M. Venetta, B. DiMassimo, G. A. Cloud, J. Y. Lee, L. Alldredge, E. Hunter, D. Lambert, D. Bolognesi, T. Matthews, M. R. Johnson, M. A. Nowak, G. M. Shaw, and M. S. Saag. 1998. Potent suppression of HIV-1 replication in humans by T-20, a peptide inhibitor of gp41-mediated virus entry. Nat. Med. 4:1302–1307.
15. Ksiazek, T. G., D. Erdman, C. S. Goldsmith, S. R. Zaki, T. Peret, S. Emery, S. Tong, C. Urbani, J. A. Comer, W. Lim, P. E. Rollin, S. F. Dowell, A. E. Ling, C. D. Humphrey, W. J. Shieh, J. Guarner, C. D. Paddock, P. Rota, B. Fields, J. DeRisi, J. Y. Yang, N. Cox, J. M. Hughes, J. W. LeDuc, W. J. Bellini, and L. J. Anderson. 2003. A novel coronavirus associated with severe acute respiratory syndrome. N. Engl. J. Med. 348:1953–1966.
16. Lambert, D. M., S. Barney, A. L. Lambert, K. Guthrie, R. Medinas, D. E. Davis, T. Bucy, J. Erickson, G. Merutka, and S. R. Petteway, Jr. 1996. Peptides from conserved regions of paramyxovirus fusion (F) proteins are potent inhibitors of viral fusion. Proc. Natl. Acad. Sci. USA 93:2186–2191.
17. Li, F., M. Berardi, W. Li, M. Farzan, P. R. Dormitzer, and S. C. Harrison. 2006. Conformational states of the severe acute respiratory syndrome coronavirus spike protein ectodomain. J. Virol. 80:6794–6800.
18. Liu, S., G. Xiao, Y. Chen, Y. He, J. Niu, C. R. Escalante, H. Xiong, J. Farmar, A. K. Debnath, P. Tien, and S. Jiang. 2004. Interaction between heptad repeat 1 and 2 regions in spike protein of SARS-associated coronavirus: implications for virus fusogenic mechanism and identification of fusion inhibitors. Lancet 363:938–947.
19. Matsuyama, S., S. E. Delos, and J. M. White. 2004. Sequential roles of receptor binding and low pH in forming prehairpin and hairpin conformations of a retroviral envelope glycoprotein. J. Virol. 78:8201–8209.
20. Matsuyama, S., M. Ujike, S. Morikawa, M. Tashiro, and F. Taguchi. 2005. Protease-mediated enhancement of severe acute respiratory syndrome coronavirus infection. Proc. Natl. Acad. Sci. USA 102:12543–12547.
21. Medinas, R. J., D. M. Lambert, and W. A. Tompkins. 2002. C-Terminal gp40 peptide analogs inhibit feline immunodeficiency virus: cell fusion and virus spread. J. Virol. 76:9079–9086.
22. Melikyan, G. B., R. J. Barnard, R. M. Markosyan, J. A. Young, and F. S. Cohen. 2004. Low pH is required for avian sarcoma and leukosis virus Env-induced hemifusion and fusion pore formation but not for pore growth. J. Virol. 78:3753–3762.
23. Netter, R. C., S. M. Amberg, J. W. Balliet, M. J. Biscone, A. Vermeulen, L. J. Earp, J. M. White, and P. Bates. 2004. Heptad repeat 2-based peptides inhibit avian sarcoma and leukosis virus subgroup a infection and identify a fusion intermediate. J. Virol. 78:13430–13439.
24. Ni, L., J. Zhu, J. Zhang, M. Yan, G. F. Gao, and P. Tien. 2005. Design of recombinant protein-based SARS-CoV entry inhibitors targeting the heptad-repeat regions of the spike protein S2 domain. Biochem. Biophys. Res. Commun. 330:39–45.
25. Nicholls, J. M., L. L. Poon, K. C. Lee, W. F. Ng, S. T. Lai, C. Y. Leung, C. M. Chu, P. K. Hui, K. L. Mak, W. Lim, K. W. Yan, K. H. Chan, N. C. Tsang, Y. Guan, K. Y. Yuen, and J. S. Peiris. 2003. Lung pathology of fatal severe acute respiratory syndrome. Lancet 361:1773–1778.
26. Nie, Y., P. Wang, X. Shi, G. Wang, J. Chen, A. Zheng, W. Wang, Z. Wang, X. Qu, M. Luo, L. Tan, X. Song, X. Yin, J. Chen, M. Ding, and H. Deng. 2004. Highly infectious SARS-CoV pseudotyped virus reveals the cell tropism and its correlation with receptor expression. Biochem. Biophys. Res. Commun. 321:994–1000.
27. Otaka, A., M. Nakamura, D. Nameki, E. Kodama, S. Uchiyama, S. Nakamura, H. Nakano, H. Tamamura, Y. Kobayashi, M. Matsuoka, and N. Fujii. 2002. Remodeling of gp41-C34 peptide leads to highly effective inhibitors of the fusion of HIV-1 with target cells. Angew. Chem. Int. Ed. Engl. 41:2937–2940.
28. Petit, C. M., J. M. Melancon, V. N. Chouljenko, R. Colgrove, M. Farzan, D. M. Knipe, and K. G. Kousoulas. 2005. Genetic analysis of the SARS-coronavirus spike glycoprotein functional domains involved in cell-surface expression and cell-to-cell fusion. Virology 341:215–230.
29. Qiu, Z., S. T. Hingley, G. Simmons, C. Yu, J. Das Sarma, P. Bates, and S. R. Weiss. 2006. Endosomal proteolysis by cathepsins is necessary for murine coronavirus mouse hepatitis virus type 2 spike-mediated entry. J. Virol. 80:5768–5776.
30. Rapaport, D., M. Ovadia, and Y. Shai. 1995. A synthetic peptide corresponding to a conserved heptad repeat domain is a potent inhibitor of Sendai virus-cell fusion: an emerging similarity with functional domains of other viruses. EMBO J. 14:5524–5531.
31. Rota, P. A., M. S. Oberste, S. S. Monroe, W. A. Nix, R. Campagnoli, J. P. Icenogle, S. Penaranda, B. Bankamp, K. Maher, M. H. Chen, S. Tong, A. Tamin, L. Lowe, M. Frace, J. L. DeRisi, Q. Chen, D. Wang, D. D. Erdman, T. C. Peret, C. Burns, T. G. Ksiazek, P. E. Rollin, A. Sanchez, S. Liffick, B. Holloway, J. Limor, K. McCaustland, M. Olsen-Rasmussen, R. Fouchier, S. Gunther, A. D. Osterhaus, C. Drosten, M. A. Pallansch, L. J. Anderson, and W. J. Bellini. 2003. Characterization of a novel coronavirus associated with severe acute respiratory syndrome. Science 300:1394–1399.
32. Sagara, Y., Y. Inoue, H. Shiraki, A. Jinno, H. Hoshino, and Y. Maeda. 1996. Identification and mapping of functional domains on human T-cell lymphotropic virus type 1 envelope proteins by using synthetic peptides. J. Virol. 70:1564–1569.
33. Simmons, G., D. N. Gosalia, A. J. Rennekamp, J. D. Reeves, S. L. Diamond, and P. Bates. 2005. Inhibitors of cathepsin L prevent severe acute respiratory syndrome coronavirus entry. Proc. Natl. Acad. Sci. USA 102:11876–11881.
34. Simmons, G., J. D. Reeves, A. J. Rennekamp, S. M. Amberg, A. J. Piefer, and P. Bates. 2004. Characterization of severe acute respiratory syndrome-associated coronavirus (SARS-CoV) spike glycoprotein-mediated viral entry. Proc. Natl. Acad. Sci. USA 101:4240–4245.
35. Supekar, V. M., C. Bruckmann, P. Ingallinella, E. Bianchi, A. Pessi, and A. Carfi. 2004. Structure of a proteolytically resistant core from the severe acute respiratory syndrome coronavirus S2 fusion protein. Proc. Natl. Acad. Sci. USA 101:17958–17963.
36. Wang, E., X. Sun, Y. Qian, L. Zhao, P. Tien, and G. F. Gao. 2003. Both heptad repeats of human respiratory syncytial virus fusion protein are potent inhibitors of viral fusion. Biochem. Biophys. Res. Commun. 302:469–475.
37. Watanabe, S., A. Takada, T. Watanabe, H. Ito, H. Kida, and Y. Kawaoka. 2000. Functional importance of the coiled-coil of the Ebola virus glycoprotein. J. Virol. 74:10194–10201.
38. Wild, C., T. Oas, C. McDanal, D. Bolognesi, and T. Matthews. 1992. A synthetic peptide inhibitor of human immunodeficiency virus replication: correlation between solution structure and viral inhibition. Proc. Natl. Acad. Sci. USA 89:10537–10541.
39. Wild, C. T., D. C. Shugars, T. K. Greenwell, C. B. McDanal, and T. J. Matthews. 1994. Peptides corresponding to a predictive alpha-helical domain of human immunodeficiency virus type 1 gp41 are potent inhibitors of virus infection. Proc. Natl. Acad. Sci. USA 91:9770–9774.
40. Xu, Y., Z. Lou, Y. Liu, H. Pang, P. Tien, G. F. Gao, and Z. Rao. 2004. Crystal structure of severe acute respiratory syndrome coronavirus spike protein fusion core. J. Biol. Chem. 279:49414–49419.
41. Yang, Z. Y., Y. Huang, L. Ganesh, K. Leung, W. P. Kong, O. Schwartz, K. Subbarao, and G. J. Nabel. 2004. pH-dependent entry of severe acute respiratory syndrome coronavirus is mediated by the spike glycoprotein and enhanced by dendritic cell transfer through DC-SIGN. J. Virol. 78:5642–5650.
42. Yao, Q., and R. W. Compans. 1996. Peptides corresponding to the heptad repeat sequence of human parainfluenza virus fusion protein are potent inhibitors of virus infection. Virology 223:103–112.
43. Young, J. K., D. Li, M. C. Abramowitz, and T. G. Morrison. 1999. Interaction of peptides with sequences from the Newcastle disease virus fusion protein heptad repeat regions. J. Virol. 73:5945–5956.
44. Yu, M., E. Wang, Y. Liu, D. Cao, N. Jin, C. W. Zhang, M. Bartlam, Z. Rao, P. Tien, and G. F. Gao. 2002. Six-helix bundle assembly and characterization of heptad repeat regions from the F protein of Newcastle disease virus. J. Gen. Virol. 83:623–629.
45. Yuan, K., L. Yi, J. Chen, X. Qu, T. Qing, X. Rao, P. Jiang, J. Hu, Z. Xiong, Y. Nie, X. Shi, W. Wang, C. Ling, X. Yin, K. Fan, L. Lai, M. Ding, and H. Deng. 2004. Suppression of SARS-CoV entry by peptides corresponding to heptad regions on spike glycoprotein. Biochem. Biophys. Res. Commun. 319:746–752.

JOURNAL OF VIROLOGY, Apr. 2008, p. 3261–3270
0022-538X/08/$08.00+0 doi:10.1128/JVI.01154-07

Vol. 82, No. 7

Amino Acid Mutation N348I in the Connection Subdomain of Human Immunodeficiency Virus Type 1 Reverse Transcriptase Confers Multiclass Resistance to Nucleoside and Nonnucleoside Reverse Transcriptase Inhibitors▽†

Atsuko Hachiya,[1,2] Eiichi N. Kodama,[3]* Stefan G. Sarafianos,[4] Matthew M. Schuckmann,[4] Yasuko Sakagami,[3] Masao Matsuoka,[3] Masafumi Takiguchi,[2] Hiroyuki Gatanaga,[1] and Shinichi Oka[1]

AIDS Clinical Center, International Medical Center of Japan, Tokyo, Japan[1]; Center for AIDS Research, Kumamoto University, Kumamoto, Japan[2]; Institute for Virus Research, Kyoto University, Kyoto, Japan[3]; and Department of Molecular Microbiology and Immunology, University of Missouri School of Medicine, Bond Life Sciences Center, Columbia, Missouri[4]

Received 28 May 2007/Accepted 9 January 2008

We identified clinical isolates with phenotypic resistance to nevirapine (NVP) in the absence of known nonnucleoside reverse transcriptase inhibitor (NNRTI) mutations. This resistance is caused by N348I, a mutation at the connection subdomain of human immunodeficiency virus type 1 (HIV-1) reverse transcriptase (RT). Virologic analysis showed that N348I conferred multiclass resistance to NNRTIs (NVP and delavirdine) and to nucleoside reverse transcriptase inhibitors (zidovudine [AZT] and didanosine [ddI]). N348I impaired HIV-1 replication in a cell-type-dependent manner. Acquisition of N348I was frequently observed in AZT- and/or ddI-containing therapy (12.5%; $n = 48$; $P < 0.0001$) and was accompanied with thymidine analogue-associated mutations, e.g., T215Y ($n = 5/6$) and the lamivudine resistance mutation M184V ($n = 1/6$) in a Japanese cohort. Molecular modeling analysis shows that residue 348 is proximal to the NNRTI-binding pocket and to a flexible hinge region at the base of the p66 thumb that may be affected by the N348I mutation. Our results further highlight the role of connection subdomain residues in drug resistance.

Combinations of multiple drugs used for clinical treatment of human immunodeficiency virus type 1 (HIV-1) infections in highly active antiretroviral therapies (HAART) can dramatically reduce viral load, increase levels of CD4positive cells, improve survival rates, and delay the onset of AIDS. HAART typically includes two nucleoside reverse transcriptase inhibitors (NRTIs) and a nonnucleoside reverse transcriptase inhibitor (NNRTI) or a protease inhibitor (17). After prolonged therapy, however, an increasing number of treatment failures are caused by the emergence of multidrug-resistant (MDR) variants. For example, treatment with zidovudine (AZT) and dideoxynuleoside RT inhibitors such as didanosine (ddI) may result in the "Q151 complex" of clinical mutations in RT (A62V/V751/F77L/F116Y/Q151M) which causes high-level resistance to multiple NRTIs, AZT, ddI, zalcitabine (ddC), and stavudine (d4T) (21, 38). Another MDR complex of RT mutations is the "fingers insertion" complex that includes an insertion of two residues at the fingers subdomain of the p66 subunit of RT in the presence of AZT resistance mutations, e.g., M41L and T215Y (M41L/T69SSG/T215Y). This complex can emerge during combination treatment that includes NRTIs (10, 41) and confers resistance to multiple drugs by enhancing the excision reaction that causes resistance by unblocking NRTI-terminated primers (40). G333E or G333D polymorphisms with thymidine analogue-associated mutations (TAMs) and M184V have also been reported to facilitate moderate resistance to at least two NRTIs, AZT and lamivudine (3TC) (7, 22). RT mutations K103N, V106M, and Y188L are associated with resistance to multiple NNRTIs (1, 5). Since all NNRTIs bind at the same hydrophobic binding pocket, mutations in the binding pocket may result in broad cross-resistance between members of this family of drugs.

The presence of variants that are resistant to multiple drugs limits significantly the available therapeutic strategies and, even more profoundly, therapeutic options. However, so far all reports of viruses that acquire resistance to members of both families of RT inhibitors describe variants with multiple mutations at several residues that confer either NRTI or NNRTI resistance. Recently, Paolucci et al. reported that Q145M/L mutations confer cross-resistance to some NRTIs and NNRTIs (31, 32). Similarly, an NNRTI resistance mutation, Y181I, also confers resistance to d4T at the enzyme level (2). The frequency of these mutations in clinical isolates does not appear to be significant, according to the Stanford HIV resistance database (http://hivdb.stanford.edu/index.html); there is no deposition for Q145M/L, and Y181I has a prevalence of 0.02% in drug-naïve or NRTI-treated patients and 0.9% in NNRTI-treated patients.

We report here that N348I is a multiclass resistance mutation involved in resistance to both NRTIs and NNRTIs and present in a significant number of clinical isolates. Residue 348 is at the RT connection subdomain outside the region usually

* Corresponding author. Mailing address: Laboratory of Virus Immunology, Research Center for AIDS, Institute for Virus Research, Kyoto University, 53, Kawaramachi, Shogoin, Sakyo-ku, Kyoto 606-8507, Japan. Phone and fax: 81 75 751 3986. E-mail: ekodama@virus.kyoto-u.ac.jp.

† Supplemental material for this article may be found at http://jvi.asm.org/.

▽ Published ahead of print on 23 January 2008.

sequenced as the drug resistance assay in clinical settings. The role of connection subdomain mutations in AZT resistance has been highlighted recently by Pathak and colleagues (28). The present work shows that N348I confers resistance not only to the NRTI AZT but also to another NRTI, ddI, and two NNRTIs, nevirapine (NVP) and delavirdine (DLV). Importantly, we show that the N348I variant emerges frequently during chemotherapy containing AZT and/or ddI. To our knowledge, this is the first example of a clinically significant and high-prevalence multiclass RTI resistance mutation that highlights the need for extensive phenotypic and genotypic assays to detect novel mutations with important implications on future therapeutic strategies.

MATERIALS AND METHODS

Reagents and cells. AZT, ddI, ddC, and d4T were purchased from Sigma (St. Louis, MO). 3TC, DLV, and tenofovir (TDF) were purchased from Moravek Biochemicals, Inc. (Brea, CA). NVP, abacavir (ABC), and efavirenz (EFV) were generously provided by Boehringer Ingelheim Pharmaceutics Inc. (Ridgefield, CT), GlaxoSmithKline (Philadelphia, PA), and Merck Co. Inc. (Rahway, NJ), respectively. Loviride was kindly provided by S. Shigeta, Fukushima Medical University (Fukushima, Japan). MT-2, SupT1, PM1, H9, Cos-7, and MAGIC-5 cells (CCR5-transduced HeLa-CD4/LTR-β-Gal cells) were cultured and used as described previously (14). Peripheral blood mononuclear cells (PBMCs) obtained from healthy donors were stimulated with phytohemagglutinin (PHA) for 3 days and grown in RPMI 1640 medium with 10% fetal calf serum and 10 U of interleukin-2 as described previously (15, 23).

Clinical isolates. Clinical isolates were obtained from fresh plasma of an HIV-1-infected patient attending the outpatient clinic of the AIDS Clinical Center, International Medical Center of Japan, using MAGIC-5 cells. The isolates were stored at −80°C until use, and infectivity was measured as blue cell-forming units (BFU) of MAGIC-5 cells. The Institutional Review Board approved this study (IMCJ-H13-80), and written informed consent was obtained from the patient.

Viruses and construction of recombinant HIV-1 clones. An HIV-1 infectious clone, pNL101, was kindly provided by K.-T. Jeang (NIH, Bethesda, MD) and used for generating recombinant HIV-1 clones (15). A wild-type (WT) HIV-1, designated HIV-1_{WT}, was constructed by replacing the *pol*-coding region (nucleotides [nt] 2006 of ApaI site to 5785 of SalI site of pNL101) with the HIV-1 BH10 strain. The *pol*-coding region contains a silent mutation at nt 4232 (TTTAGA to TCTAGA; mutation is italicized) for generation of an XbaI unique site. The DNA fragments amplified by reverse transcription-PCR from the primary isolates were digested with appropriate restriction enzymes and cloned into pNL-RT_{WT}. The nucleoside sequences of the PCR-amplified fragments were verified with a model 3730 automated DNA Sequencer (Applied Biosystems, Foster, CA). Viral stocks were obtained by transfection of each molecular clone into Cos-7 cells, harvested, and stored at −80°C until use.

Sequencing analysis of HIV-1 RT region. Viral RNA was extracted from plasma and/or culture supernatant of clinical isolates and subjected to reverse transcription-PCR using a OneStep RNA PCR Kit (Takara Bio, Otsu, Japan). Nested PCR was subsequently conducted for direct sequencing. Primer pairs used for amplification of the DNA fragment from nt 2574 to 3333 of pNL101 were T1 (5′-AGGGGGAATTGGAGGTTT; nt 2393 to 2410) and T4 (5′-TTCT GTTAGTGCTTTGGTT; nt 3422 to 3404) for the first PCR and T12 (5′-CCAG TAAAATTAAAGCCAG; nt 2574 to 2592) and T15 (5′-TCCCACTAACTTCT GTATGTC; nt 3335 to 3315) for the second PCR (15). Primer pairs used for amplification of DNA fragment from nt 3288 to 4316 were 3244F (5′-AT GAACTCCATCCTGACAAATG; nt 3244 to 3265) and 4428R (5′-TGTA CAATCTAATTGCCATAT; nt 4428 to 4407) for the first PCR and 3288F (5′-CCAGAAAAAGACAGCTGGACT; nt 3288 to 3308) and 4316R (5′-TG GCAGATTAAAATCACTAGCC; nt 4316 to 4295) for the second PCR (13). The nested PCR products were then subjected to the direct sequencing of the entire RT coding region, and some PCR products were further analyzed with clonal sequence determination as described previously (13, 15).

Drug susceptibility assay. HIV-1 sensitivity to various RTIs was determined in triplicate using MAGIC-5 cells as described previously (14). MAGIC-5 cells were infected with diluted virus stock (100 BFU) in the presence of increasing concentrations of RTIs, cultured for 48 h, fixed, and stained with X-Gal (5-bromo-4-chloro-3-indolyl-βD-galactopyranoside). The stained cells were counted under a light microscope. Drug concentrations reducing the cell number to 50% of that of the drug-free control (EC_{50}) were determined by referring to the dose-response curve.

Competition assay of HIV-1 replication. MT-2, SupT1, PM1, and H9 cells (2.5×10^5 cells/5 ml) and PHA-stimulated PBMCs (2.5×10^6 cells/5 ml) were infected with each virus preparation (500 BFU) for 4 h. The infected cells were then washed and cultured in a final volume of 5 ml. Culture supernatants (100 μl) were harvested from days 1 to 7 after infection, and the p24 antigen amounts were quantified (27).

Freshly prepared H9 cells (3×10^5 cells/well) were exposed to the mixture of viral preparations (300 BFU) and cultured to compare their replicative capacities, as previously described (15). On day 1 in culture, one-third of the infected H9 cells were harvested and washed twice with phosphate-buffered saline, followed by DNA extraction. Purified DNA was subjected to nested PCR to sequence the HIV-1 RT genes. The supernatant of the viral culture was transferred to uninfected H9 cells at 7-day intervals, and the cells harvested at each passage were subjected to direct DNA sequencing of the HIV-1 RT gene. Population change of the viral mixture was determined by the relative peak height on the sequencing electrogram. The persistence of the original amino acid substitution was confirmed in all infectious clones used in this assay.

Molecular modeling studies. The SYBYL and O programs were used to prepare molecular models of the complexes of WT and N348I HIV-1 RT with DNA, NVP, and the triphosphates of AZT and ddI. Starting atomic coordinates of HIV-1 RT in complex with DNA were obtained from the structures described by Tuske et al. (40), Sarafianos et al. (36), and Huang et al. (20) (Protein Data Bank [PDB] code numbers 1T05, 1N6Q, and 1RTD, respectively). Because there is no available structure of RT in complex with both NNRTI and DNA, we used structures of RT in complex with NNRTI to obtain initial coordinates of the NNRTI-binding pocket (9, 12). Specifically, we used the coordinates of the two β-sheets of the polymerase active site (β6-β9-β10 that contains the three catalytic aspartates and the YMDD motif as well as β12-β13 of the primer grip) to replace the corresponding regions in the RT-DNA complex. The N348I side chain mutation was manually modeled in the p66 subunit, and all structures were optimized using energy minimization protocols in SYBYL. The triphosphates of AZT and ddI were built based on the structures of AZT monophosphate and dTTP in PDB 1N6Q (36) and 1RTD (20) or of TDF diphosphate in the ternary complex of HIV-1 RT/DNA/TFV-DP, PDB 1T03 (40). The coordinate vector of the resulting structures was varied using a minimization procedure to minimize the potential energy by relieving short interatomic distances while maintaining structural integrity.

RESULTS

Resistance to NNRTIs observed in HIV-1 isolates. The clinical history of the patient is summarized in Fig. 1 and includes the variation of genotypic and phenotypic drug resistance profiles of sequential isolates with time (see also Table S1 and Fig. S1 in the supplemental material). In spite of the combination therapy, little immunologic and virologic response was observed; at time point 2, the CD4 count was 25/μl, and the plasma HIV-1 RNA levels were 2.1×10^6 copies/ml. However, no known drug resistance mutations associated to both NRTIs and NNRTIs were detected in the RT region at this point (Fig. 1B). Due to poor adherence, upon changing the regimen we observed only partial suppression of viral replication and limited increase in the CD4 count. TAMs with N348I accumulated during time points 3 to 6 (Fig. 1). In February 2000, the treatment was interrupted due to severe adverse effects, resulting in a rebound of viral load. In July 2000, the same therapy was resumed for approximately 1 year. No drug resistance-associated mutations were detected upon initiation of this therapy (time point 7). At time point 8, mixtures of two amino acid insertions at codon 69 with TAMs and N348I were detected, although these mutations disappeared after the treatment interruption at time point 10.

Interestingly, HIV-1 isolates at time points 5 and 6 showed resistance to NVP (44- and 25-fold, respectively) and to DLV

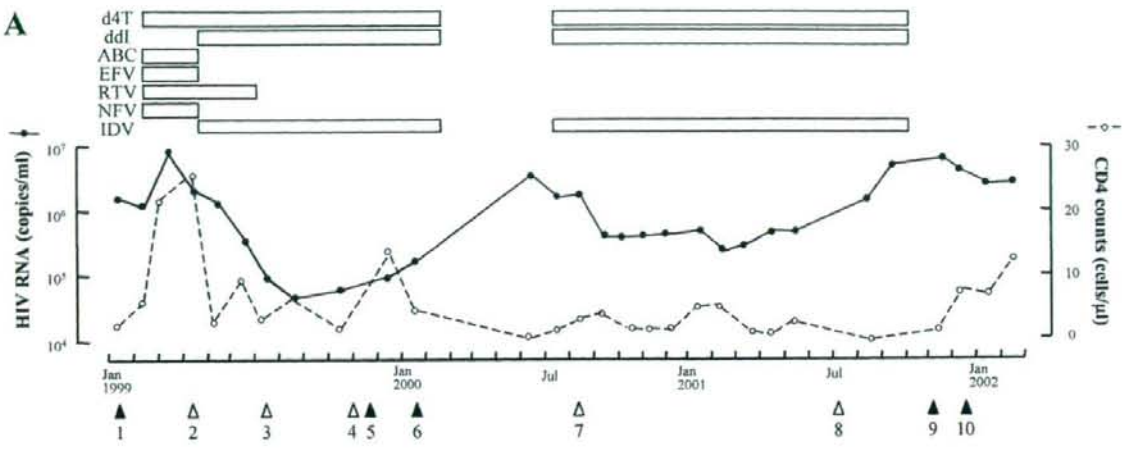

B

Time point	Resistance-associated and unique mutations											Fold increase in EC_{50}								
	M41	D67	T69	K70	V75	V118	L210	T215	L283	N348	I393	AZT	ddI	ddC	d4T	3TC	ABC	NVP	DLV	EFV
1	-	-	-	-	-	-	-	-	I	-	L	2	1.5	0.6	1.0	0.9	0.8	2.2	1	1
2	-	-	-	-	-	-	-	-	I	-	L					N.D.				
3	M/L	-	-	-	-	-	-	-	I	-	L					N.D.				
4	L	N	-	-	M	-	W	Y	I	N/I	L					N.D.				
5	L	N	-	-	M	-	W	Y	I	I	L	**44**	**4.3**	0.6	1.8	1.6	1.6	**44**	**8.5**	**3**
6	L	N	-	-	M	I	W	Y	I	I	L	**275**	**5.9**	2.5	**3.2**	**3.4**	2	**25**	**12**	1
7	-	-	-	-	-	-	-	-	I	-	L					N.D.				
8	L	T/N	-/SSG	E	M	I	W	Y	I	N/I	L					N.D.				
9	-	-	-	-	V/M	V/I	L/W	T/Y	I	-	-	2	1.2	0.6	1.1	0.6	1	2.4	1.5	0.7
10	-	-	-	-	-	-	-	-	I	-	-	2.8	0.7	0.6	1	0.8	1.2	1.8	1	1

FIG. 1. The course of patient and drug resistance profiles of clinical isolates obtained from the patient. (A) The drug treatment history is indicated at the top of the graph. The virologic responses represented by plasma viral load and CD4 counts of peripheral blood are shown. Open triangles indicate the time points of genotypic assays. Closed triangles indicate the time points of isolation of clinical isolates for genotypic assays (also see Fig. S1 in the supplemental material) and phenotypic assays (also see Table S1 in the supplemental material showing actual EC_{50} values as mean values and standard deviations from three independent experiments). From February to June 2000 and after October 2001, the chemotherapy was interrupted due to severe adverse effects. (B) The viruses acquired NRTI resistance mutations sequentially as shown. Susceptibility to compounds tested in at least three independent experiments is shown as the relative increase in the EC_{50} compared to HIV-1_{WT} obtained from a pNL4-3-based plasmid. An increase larger than 3.0-fold is indicated in bold. NRTI or NNRTI resistance mutations were reported in the HIV drug resistance database maintained by International AIDS Society 2006, the Stanford University (Stanford, CA) and Los Alamos National Laboratory (Los Alamos, NM), http://hivdb.stanford.edu/and http://resdb.lanl.gov/Resist_DB/, respectively. RTV, ritonavir; NFV, nelfinavir; IDV, indinavir.

(8.5- and 12-fold, respectively) but lacked any known NNRTI resistance-associated mutations except for L283I, which influences susceptibility of NNRTIs when combined with I135L/M/T (6) (Fig. 1B). However, L283I was detected at all points without I135L/M/T even in phenotypically sensitive viruses; therefore, it is unlikely that this single mutation is involved in the resistance. After the interruption at time points 9 and 10, the majority of HIV-1 detected in the plasma reverted to WT and was susceptible to all RTIs tested. The patient was previously treated with a regimen containing EFV, not NVP, for several months prior to the appearance of the N348I mutation. Importantly, this mutation was not detected in genotypic assays during treatment with EFV, but it was first detected 6 months after removal of EFV and use of ddI in the following regimen. Phenotypic and genotypic information at time point 5 shows that resistance to NVP and DLV was present while the patient was on a regimen that did not include any NNRTIs and in the absence of any known NNRTI resistance-related mutations. Thus, it is unlikely that the phenotypically identified NNRTI resistance in the patient was induced by the previous EFV-containing therapy.

RT C-terminal region confers NVP resistance. To identify the mutation(s) responsible for the resistance to NVP and DLV, we constructed chimeric clones with cDNA fragments of the RT region derived from the clinical isolates. Briefly, the N-terminal (amino acids 15 to 267) and C-terminal (amino acids 268 to 560) RT coding regions of clinical isolates were PCR amplified separately and used for replacement of the corresponding regions in the WT sequence of pNL-RT_{WT}. These chimeric clones were then examined for their susceptibility to RTIs (Table 1). Only the clones containing the C-terminal region derived from CL-6 isolated at time point 6 and

TABLE 1. Susceptibility of chimeric HIV-1 clones with N- and/or C-terminal RT region substitutions

RT-replaced region		EC_{50} (fold increase)[a]				
N terminus[b]	C terminus[c]	AZT	ddI	NVP	DLV	EFV
WT[d]	WT	0.038 ± 0.012	2.6 ± 1.04	0.05 ± 0.01	0.03 ± 0.01	0.003 ± 0.001
CL-6[e]	CL-6[e]	3.37 ± 0.97 (**89**)	14.3 ± 0.58 (**5.5**)	1.2 ± 0.21 (**24**)	0.16 ± 0.02 (**5.3**)	0.007 ± 0.004 (2.3)
CL-9[f]	CL-9[f]	0.04 ± 0.01 (1.1)	2.3 ± 1.21 (0.9)	0.13 ± 0.07 (2.6)	0.06 ± 0.02 (2)	0.004 ± 0.002 (1.3)
CL-6	WT	1.24 ± 0.34 (**33**)	4.6 ± 1.50 (1.8)	0.12 ± 0.06 (2)	0.04 ± 0.02 (1.3)	0.002 ± 0.001 (0.7)
WT	CL-6	0.19 ± 0.04 (**5**)	13.7 ± 2.31 (**5.3**)	1.67 ± 0.23 (**33**)	0.39 ± 0.06 (**13**)	0.006 ± 0.002 (2)
CL-6	CL-9	1.50 ± 0.95 (**39**)	5.9 ± 1.21 (2.3)	0.10 ± 0.05 (2)	0.04 ± 0.02 (1.3)	0.002 ± 0.001 (0.7)

[a] The data shown are mean values ± standard deviations obtained from the results of at least three independent experiments, and the relative increase in the EC_{50} values for recombinant viruses compared with WT is shown in parentheses. Bold indicates an increase in EC_{50} value greater than threefold relative to the WT.
[b] RT N-terminal region contains mainly the domains of finger and palm and partially thumb (amino acid positions 15 to 267).
[c] RT C-terminal region contains domains of thumb, connection, and RNase H (amino acid positions 268 to 560).
[d] DNA fragment is identical to pNL-RT_{WT}.
[e] N- and C-terminal regions of CL-6 contained T39A/M41L/K43E/D67N/V75M/V118I/I132V/L210W/T215Y and N348I/I393L in their coding regions, respectively (see also Fig. S1 in the supplemental material).
[f] No resistance-associated mutations were observed in either the N- or C-terminal region of CL-9 (also see Fig. S1 in the supplemental material).

showed resistance (Fig. 1; see also Fig. S1 in the supplemental material) to NVP and DLV. Interestingly, the C-terminal region also conferred resistance to AZT and ddI even in the absence of AZT resistance mutations that normally reside at the N-terminal region within amino acids 41 to 219. Recently, mutations in the connection subdomain, including G335D, N348I, and A360T, have been shown to confer AZT resistance (28). In these clinical isolates the C-terminal region contained four unique mutations in the connection subdomain: G335D, N348I, A360T, and I393L (see Fig. S1 in the supplemental material). G335D and A360T were continuously observed at every time point and are polymorphisms related to subtype D. Since these isolates showed no phenotypic resistance (Table 1 and Fig. 1B), it is unlikely that G335D and A360T are involved in the resistance, at least in subtype D. I393L was also continuously detected from time point 1 but disappeared after the treatment interruption at time point 9 (Fig. 1) while N348I appeared only from time points 4 to 6 and at point 8 under treatment.

To further clarify the effect of mutations at residues 348 and 393 on drug resistance, we generated the N348I and/or I393L mutations in the C-terminal region by site-directed mutagenesis on a pNL-RT_{WT} background. Consistent with the phenotypic experiments and the experiments with chimeric viruses, we found that the N348I substitution conferred resistance to AZT, ddI, NVP, and DLV. In contrast, we found that the I393L mutation caused no significant resistance by itself (Table 2). Furthermore, the combination of I393L with N348I did not show any significant increase in NVP resistance compared to N348I alone.

To address whether N348I further increases the level of AZT resistance in the presence of TAMs, we examined the effect of N348I on AZT susceptibility in the presence or absence of the classical AZT resistance mutations M41L/T215Y. M41L/T215Y or N348I showed only moderate resistance to AZT whereas a combination of M41L/T215Y and N348I further enhanced AZT resistance (Table 2). These data demonstrate that the N348I mutation is responsible for this cross-resistance to multiple members of the NRTI and NNRTI families and enhances AZT resistance induced by TAMs.

Viral replication kinetics. Since N348I and I393L immediately disappeared after cessation of HAART, we examined whether these mutations have an effect on viral replication kinetics using the p24 antigen production assay and a competitive HIV-1 replication assay (CHRA). In the p24 antigen production assay, acquisition of N348I drastically impaired replication in MT-2 and SupT1 cells (Fig. 2A and B). However, a moderately low reduction of replication kinetics was observed in PM1, H9 cells, and PHA-stimulated PBMCs (Fig. 2C, D, and E). HIV-1 carrying the mutation I393L (HIV-1_{I393L}) showed comparable replication kinetics in all cells tested. A combination of I393L with N348I showed no apparent change of replication kinetics in MT-2, SupT1 cells, and PHA-stimulated PBMCs (Fig. 2A, B, and E) and reduction in PM1 cells (Fig. 2C) compared to N348I alone. CHRA was performed for further comparison of replication kinetics in H9 cells. During 6 weeks in culture, we observed little difference in viral replication in H9 cells (Fig. 2F). A lack of an effect of I393L on the replication of N348I was confirmed by CHRA (Fig. 2G). These results indicate that N348I impairs viral replication in a cell-type-dependent manner and that I393L exerts little effect on viral replication of either the WT or N348I clones. Thus, I393L appears to be one of the specific polymorphisms for this isolate.

Insertion at 69 and N348I. At time point 8 we detected the transient presence of the fingers insertion mutation, a 2-amino-acid insertion at codon 69 in the presence of TAMs known to confer resistance to NRTIs by enhancing the excision reaction (3) (Fig. 1). Interestingly, at time point 8 WT N348 coexisted with resistant I348. To address whether these two MDR mutations were introduced onto the same RNA genome, we carried out clonal sequence analysis of PCR products. The results show that the fingers insertion and the N348I mutations were randomly introduced; seven, three, one, and six clones ($n = 17$) contained both mutations, the fingers insertion only, N348I only, and no mutation or insertion, respectively, in the background of TAMs (Table 3). In previous studies the fingers insertion complex emerged with the K70E mutation that was selected in vitro with adefovir (8) and β-2′,3′-didehydro-2′,3′-dideoxy-5-fluorocytidine (18), and it conferred low level resistance to TDF, ABC, and 3TC (39). The effect of K70E on resistance or enzymatic activity influenced by the fingers insertion remains to be elucidated. These results suggest that there is no correlation between the N348I and the

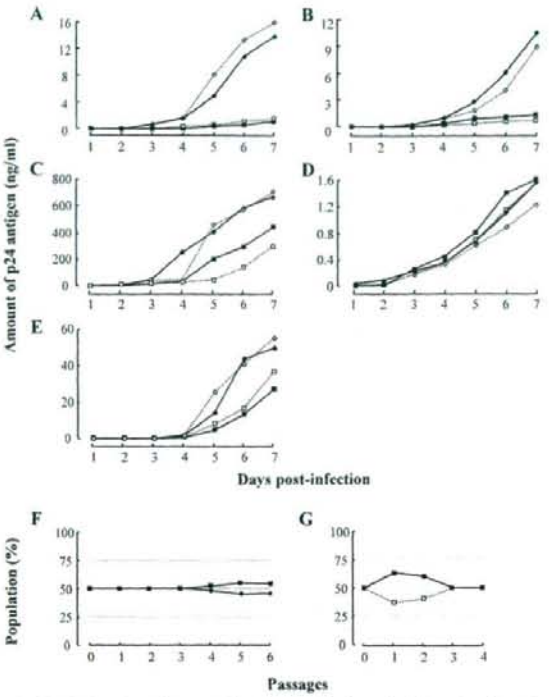

FIG. 2. Viral replication kinetics. Production of p24 antigen in culture supernatant was determined with a commercially available p24 antigen kit. Profiles of replication kinetics (p24 production) of HIV-1_{WT} (closed diamonds), HIV-1_{N348I} (closed squares), HIV-1_{I393L} (open diamonds) and HIV-$1_{N348I/I393L}$ (open squares) were determined with MT-2 (A), SupT1 (B), PM1 (C) and H9 cells (D) and PHA-stimulated PBMCs (E). Representative results from at least two (or three) independent single determinations of p24 production with newly titrated viruses are shown. A competitive HIV-1 replication assay was performed in H9 cells to compare the replication kinetics of HIV-1_{WT} (closed diamond) and HIV-1_{N348I} (closed squares) (F) and of HIV-1 N348I (closed squares) and HIV-$1_{N348I/I393L}$ (open square) (G).

finger insertion mutations. Because our studies show that N348I does not confer d4T resistance, we speculate that the fingers insertion mutation was introduced to overcome the drug pressure by d4T.

TABLE 3. Sequences of HIV-1 RT-coding region of clinical samples

No. of clones[a]	Resistance-associated and unique mutation at the indicated position									
	M41	D67	T69	K70	V75	V118	L210	T215	N348	I393
5	L	N			M	I	W	Y		L
3	L	T	SSG	E	M		W	Y	I	L
3	L	T	SSG	E	M	I	W	Y	I	L
2	L	T	SSG	E			W	Y		L
1	L	T	SSG	E			W	Y	I	L
1	L	T	SSG	E	M	I	W	Y		L
1	L				M					
1	L				M	I	W	Y	I	L

[a] The PCR product at time point 8 was subcloned and sequenced (n = 17).

TABLE 2. Drug susceptibilities of HIV-1 variants constructed by site-directed mutagenesis

Mutation[a]	EC_{50} (fold increase)[b]											
	NRTI							NNRTI				
	AZT	ddI	ddC	d4T	3TC	ABC	TDF	NVP	DLV	Lowride	EFV	
WT	0.035 ± 0.01	2.3 ± 0.14	0.7 ± 0.13	3.6 ± 1.36	2.1 ± 0.2	3.4 ± 0.14	0.03 ± 0.01	0.04 ± 0.02	0.04 ± 0.01	1.4 ± 0.38	0.003 ± 0.0008	
N348I	0.24 ± 0.04 (6.9)	12 ± 1.0 (5.2)	0.74 ± 0.58 (1.1)	2.9 ± 0.21 (0.8)	1.7 ± 0.36 (0.8)	3.4 ± 1.11 (1)	0.02 ± 0.01 (0.7)	1.07 ± 0.06 (27)	0.22 ± 0.04 (5.5)	2.4 ± 0.35 (1.7)	0.005 ± 0.0005 (1.7)	
I393L	0.06 ± 0.01 (1.7)	2 ± 1.37 (0.9)	0.42 ± 0.23 (0.6)	1.8 ± 1.21 (0.5)	1.5 ± 0.74 (0.7)	2.4 ± 0.95 (0.7)	0.02 ± 0.01 (0.7)	0.05 ± 0.01 (1.3)	0.04 ± 0.01 (1.0)	2.2 ± 0.4 (1.6)	0.003 ± 0.001 (1)	
N348I/I393L	0.23 ± 0.03 (6.6)	11.3 ± 1.53 (4.9)	0.49 ± 0.01 (0.7)	4.2 ± 1.12 (1.2)	1.7 ± 0.40 (0.8)	2.7 ± 0.26 (0.8)	0.02 ± 0.01 (0.7)	1.02 ± 0.51 (26)	0.28 ± 0.06 (7)	2.6 ± 0.42 (1.8)	0.005 ± 0.001 (1.7)	
M41L/T215Y	0.28 ± 0.06 (8)	4.5 ± 1.55 (2)	ND	ND	1.3 ± 0.25 (0.6)	ND	ND	0.05 ± 0.01 (1.3)	0.04 ± 0.02 (1)	ND	0.002 ± 0.0004 (0.7)	
M41L/T215Y/ N348I	1.37 ± 0.21 (39)	9.9 ± 0.99 (4.3)	ND	ND	1.4 ± 0.20 (0.7)	ND	ND	1.11 ± 0.69 (28)	0.15 ± 0.06 (3.8)	ND	0.002 ± 0.0004 (0.7)	

[a] See Materials and Methods for the construction of clones.

[b] Data are means ± standard deviations from at least three independent experiments. The relative increase in the EC_{50} value compared with that in HIV-1_{WT} is given in parentheses. Boldface indicates an increase greater than threefold. ND, not determined.

TABLE 4. Frequency of N348I acquisition in clinical isolates

Treatment group	No. of isolates (%)		*P* value[a]
	Total in group	With N348I	
AZT and/or ddI	48	6 (12.5)	<0.0001
AZT	22	2 (9.1)	0.011
ddI	16	2 (12.5)	0.006
AZT/ddI	10	2 (20)	0.002
Control	183	0	
Antiretrovirals with neither AZT nor ddI	55	0	
No antiretrovirals	128	0	
Deposited in Los Alamos database	328	3 (0.9)	0.0002

[a] The *P* value was determined by the Fisher's exact test. For the AZT and/or ddI treatment groups, values were compared with the control group. The P value for isolates deposited in the Los Alamos database was determined based on a comparison with the AZT and/or ddI treatment group.

Prevalence of N348I. We obtained viral specimens from 231 infected patients who visited our clinical center from May 1997 to July 2003 and analyzed HIV-1 sequences by direct sequencing (Table 4). The viral specimens were classified in two groups: (i) those from patients treated with AZT and/or ddI ($n = 48$) and (ii) those from patients treated by regimens with neither AZT nor ddI (control group, $n = 183$). The group treated with AZT and/or ddI was further divided into three subgroups based on the treatment received: with AZT, with ddI, and with the AZT/ddI combination (Table 4). During chemotherapy containing AZT ($n = 22$), ddI ($n = 16$), or the combination of AZT and ddI ($n = 10$), two patients each harbored HIV-1 with the N348I mutation. Acquisitions of N348I in all of the subgroups was statistically significant ($P = 0.011$, 0.006, and 0.002, respectively). In contrast, none of the patients in the control group ($n = 183$) harbored N348I variants. Only three variants with N348I are deposited in the Los Alamos HIV sequence database that includes subtypes B, D, and CRF14 (http://www.hiv.lanl.gov/content/hiv-db/mainpage.html). Thus, prevalence of N348I was statistically significant in the group treated that received chemotherapy containing AZT and/or ddI ($P < 0.0001$).

Because at present the numbers of NVP- or DLV-containing regimens without AZT and/or ddI are limited in our cohort ($n = 6$ or $n = 0$, respectively), we were not able to detect acquisition of N348I in these groups. Acquisition of N348I was observed in two patients treated with EFV (Table 5). Notably, these two patients were simultaneously treated with AZT and ddI, suggesting that the significance of EFV treatment for the emergence of N348I remains unknown.

Profiles of patients infected with HIV-1 containing the N348I mutation. We further analyzed the profiles of HIV-1

TABLE 5. Profiles of patients infected with HIV-1 containing the N348I mutation

Patient	Subtype of RT region[a]	Antiretroviral treatment	Duration (mo)	HIV RNA (copies/ml)	N348I	RT mutation(s) by region	
						Polymerase subdomain	Connection subdomain[d]
Case 1[b]	D	d4T, ddI, IDV	6	6.1×10^4	+/−	M41L, D67N, V75M, L210W, T215Y	G335D, A360T
		d4T, ddI, IDV	7	ND[c]	+	M41L, D67N, V75M, L210W, T215Y	G335D, A360T
Case 2	B	AZT, ddC, NFV	1	7.9×10^3	−		A360T
		AZT, ddC, NFV	4	9×10^3	−		A360T
		AZT, ddC, NFV	6	1.2×10^4	+/−	T215N/S/Y	A360T
		AZT, ddC, NFV	10	3.5×10^4	+	D67N, K70R, T215Y[e]	A360T
		d4T, 3TC, RTV, SQV	8	<50	ND	ND	ND
Case 3	B	AZT, 3TC, RTV, SQV	7	3.5×10^5	−		A360T, A376T
		AZT, 3TC, RTV, SQV	8	1.9×10^5	+	M41L, D67N, T69D, M184V, L210L/W, T215Y	A360T, A376T
		None (interruption)	7	1.2×10^5	+	M41L, D67N, T69D, M184M/V, L210L/W, T215Y	A360T, A376T
		ABC, EFV, RTV	3	60	ND	ND	ND
Case 4	B	AZT, 3TC, ddI, EFV	3	1.7×10^3	+	M184V	
Case 5	B	d4T, ddI, RTV, SQV	23	9.9×10^3	+	M41L, L210W, T215Y	
		AZT, ddI, RTV, SQV	3	6.3×10^4	+	M41L, T69D, L210W, T215Y, K219R	
		None (interruption)	7	1.8×10^5	−		
		ABC, TDF, LPV, EFV	7	<50	ND	ND	ND
Case 6	B	AZT, ddI, EFV	3	180	−		ND
		AZT, ddI, EFV	5	540	+/−	T215T/Y	ND
		AZT, ddI, EFV	6	1.1×10^4	+	T215Y	
		None (interruption)	2	2.4×10^5	−		
		d4T, 3TC, LPV	8	<50	ND	ND	ND

[a] The RT regions were sequenced and subjected to subtype analysis (http://www.ncbi.nlm.nih.gov/projects/genotyping/formpage.cgi).
[b] This patient is described in this study.
[c] ND, not detectable.
[d] G335D is an observed polymorphism in subtype D. A360I/V and A376S were reported to be AZT-resistant mutations (24).
[e] Phenotype assays were performed at 10 months for a regimen combining ddC, AZT, and NFV; resistance to AZT, ddI, and NVP was induced 52-, 6.8-, and 8.3-fold, respectively.

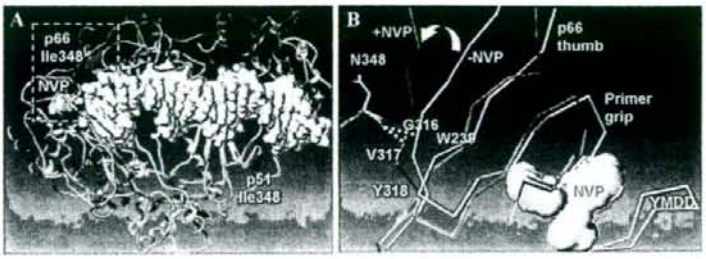

FIG. 3. Location of N348I in the modeled HIV-1 RT with NVP. (A) The N348I mutation (blue Van Der Waals volume) is shown in the connection subdomains of both p66 (purple) and p51 (cyan) subunits. The 348 residue of the p51 subunit is distant from the nucleic acid, shown as yellow Van Der Waals surfaces. In the p66 subunit (purple) the 348 residue is in a position to affect the flexibility of the p66 thumb, which in turn might affect binding of the nucleic acid. NVP is shown bound at the NNRTI binding pocket (red Van Der Waals volume). Magnification of the frame area of the enzyme is shown in panel B. (B) The main chain C=O of N348 is shown to interact with the N-H of 317 (yellow broken line) through a hydrogen bond interaction. Binding of NVP (white ball) repositions the p66 thumb subdomain with respect to (i) the polymerase active site (β6-β9-β10) that contains the three catalytic aspartates and the YMDD motif and (ii) the primer grip (β12-β13) of p66. The movement of the thumb subdomain is in a hinge-like motion that is based at the position where residue 348 interacts with residue 317.

with N348I from the six infected patients described in Table 4. The results of this analysis are shown in Table 5. The RT regions were sequenced and subjected to analysis with the software Genotyping, which uses the BLAST algorithm to determine homologies with known subtypes (http://www.ncbi.nlm.nih.gov/projects/genotyping/formpage.cgi). HIV-1 variants in case 1 belonged to subtype D, and the others belonged to subtype B. All six patients received therapy containing AZT and/or ddI. Among them, two patients (cases 4 and 6) were under therapy with EFV. However, none of them was treated with NVP or DLV. The five N348I-containing variants were in the presence of TAMs that emerged during the therapies. TAMs in case 1 and some TAMs (M41L, L210W, and T215Y) in case 5 seemed to be induced by d4T, not by AZT. In case 3, the 3TC resistance mutation M184V that attenuates TAM-induced AZT resistance (24) was present together with N348I. Similarly, in case 4, M184V may confer AZT hypersusceptibility. In case 6, N348I was present together with a classical AZT resistance mutation, T215Y. Thus, except for case 5, even under AZT-containing therapy, the HIV-1 resistance level to AZT and ddI seemed to be intermediate and weak, respectively. Additionally, viral load in cases 2, 3, 5, and 6 dramatically decreased after introduction of a new regimen without AZT and/or ddI. These results indicated that N348I may enhance AZT resistance and at least act as a primary mutation for ddI.

In these six patients, HIV-1 with the G335D mutation was observed only in case 1. In the Los Alamos HIV sequence database, G335D has been observed in 77% of subtype D HIV-1 isolates ($n = 35$). A360T was detected in two isolates of subtype B and one isolate of subtype D and was observed in 13 and 51% of drug-naïve isolates of subtypes B and D, respectively. This suggests that A360T is also one of the polymorphisms. The A360V or A360I mutation has been reported to have a modest effect on AZT resistance (28). Meanwhile, none of N348I-containing subtype B variants ($n = 5$) had mutations associated with AZT resistance in the connection subdomain (28) (Table 5).

Molecular modeling. Residue 348 is located close to the hinge site of the thumb subdomain. Mutations at the virus level affect both subunits of RT. Figure 3 shows that residue 348 of the p51 subunit is located remotely from the polymerase active site (~60 Å) and from the NNRTI binding pocket (~55 Å). Furthermore, it is not in close proximity to the interface of the two subunits (~20 Å) or the DNA in the nucleic acid binding cleft (~15 Å). On the other hand, residue 348 of the p66 subunit is proximal to the NNRTI-binding site and the nucleic acid binding cleft. These relative distances suggest that it is more likely that the interactions involve mainly residue 348 of the p66 subunit. Subunit-specific biochemical analysis would determine the precise contribution of the N348I mutation in each subunit to the drug resistance phenotype. In the p66 subunit, the main chain of the 348 residue interacts through a hydrogen bond with the main chain of V317 of the p66 thumb subdomain (Fig. 3). To determine the degree of flexibility of this part of the structure of RT, we superposed 23 structures of RT complexes. The comparison revealed measurable differences. The length of the amide bond between the main chain C=O of residue 348 and N-H of V317 varies considerably (from 2.5 to 3.6 Å), suggesting a flexibility at the junction of the connection, thumb, and palm subdomains. It is likely that the N348I mutation affects the interactions of this residue with a number of neighboring residues. In the RT/DNA/deoxynucleoside triphosphate or RT/DNA/TDF structures of ternary catalytic complexes (PDB code 1RTD or 1T05, respectively), the change of N348 to a more hydrophobic Ile would improve the hydrophobic interactions with T351 of the p66 connection subdomain and with G316 and I270 of the p66 thumb subdomain. In other structures of complexes of RT with various NNRTIs (PDB codes 1S1X, 1S6P, 1S1U, 1S1T, 1S1W, 1TKZ, 1TKX, 1TL1, 1SUQ, 1SV5, 1HNI, 1HQU, and 1HNV), residue W239 appears to be in the vicinity of these residues and likely to be affected directly or indirectly by the N348I mutation. Notably, residue W239 interacts through P-P interactions with Y318, which has been involved in resistance to NNRTIs (NVP and DLV) (19, 33).

DISCUSSION

Two previous reports have shown that two rare mutations, Q145M/L and Y181I, can confer cross-resistance to some NRTIs and NNRTIs (31, 32). N348I appears to be the first reported high-prevalence amino acid mutation to confer resistance to multiple members of the NRTI and NNRTI families. N348 is highly conserved in HIV-1 strains, including subtype O. Interestingly, the equivalent residue in HIV-2 and other retroviruses is an isoleucine (Los Alamos Sequence Data Base, http://hiv-web.lanl.gov/content/hiv-db/). Similarly, WT HIV-2 RT resembles NNRTI-resistant HIV-1 RTs at the NNRTI binding pocket region, e.g., V/I at 181 and L at 188 (34). Any of these differences from the HIV-1 enzyme, including N348I, may contribute to the observed NNRTI resistance of the HIV-2 RT. The significance and role of I348 in the natural resistance of HIV-2 to NNRTIs and susceptibility to NRTIs remain to be elucidated by further experiments.

Recently, Shafer et al. proposed criteria for evaluating the relevance of mutations to drug resistance based on extensive resistance surveillance data (37). In this review the mutations related to drug resistance were assessed by the following: (i) correlations between a mutation and treatment (whether the drug therapy selects for the mutation), (ii) correlations between a mutation and decreased in vitro drug susceptibility, and (iii) correlations between a mutation and a diminished in vivo virologic response to a new antiretroviral regimen.

Regarding the first criterion, we showed that the N348I mutation was induced by AZT and/or ddI treatment (Table 4). For the second criterion, we showed that N348I decreases susceptibility to AZT, ddI, NVP, and DLV (Table 2). The AZT and ddI resistance of the N348I clone was comparable to that of M41L/T215Y and L74V, respectively. Additionally, N348I showed 27-fold increased resistance to NVP. Regarding the third criterion, our data on patient viral load levels shown in Table 5 indicate that N348I affected the clinical outcome. Specifically, in case 6, the viral load clearly increased upon acquisition of N348I. Moreover, dramatic decreases in viral load were observed after introduction of a new regimen without AZT and/or ddI, especially in cases 2, 3, 5, and 6. Hence, the N348I mutation meets the accepted criteria for being a drug resistance mutation.

At present, it is not possible to accurately compare the incidence of N348I with that of other resistance mutations. Genotypic analysis of the largest and most recent drug resistance surveillance examined 6,247 patients treated with well-characterized RTIs, mainly performed within amino acids 1 to 240 of the RT region (35). In this surveillance, the incidences of the Q151M complex and fingers insertion were 2.6 and 0.5%, respectively. Because the connection subdomain is located outside the region sequenced in the majority of genotypic assays, only limited data are available for connection subdomain mutations such as G333E/D and N348I. Nonetheless, the incidence of N348I in our cohort is higher than other MDR mutations such as that of the Q151M complex and the insertion mutations. Furthermore, prevalence of N348I in a Canadian cohort (11.3%) (42) is comparable to that in our Japanese cohort.

In the patient case presented in Fig. 1, there is strong evidence that N348I was not present during and at least 6 months after cessation of NNRTI-based therapy. Still, because of the limited number of such cases in our cohort, it remains unclear if N348I can be induced by NNRTI-containing regimens. According to the Stanford HIV drug resistance database, the incidence of N348I in patients treated with NNRTIs is 5.8% (n = 13/224), significantly higher than in the untreated group (0.1%; n = 2/1095, $P < 0.0001$). We report here that N348I confers significant and moderate resistance to NVP and DLV, respectively. Most recently, Yap et al. also reported that combined treatment with AZT and NVP was associated with increased risk in the emergence of N348I (42). They mention that other mutations, e.g., K103N, may further enhance N348I-induced resistance to EFV. Thus, it is possible that HIV-1 also acquires N348I under NNRTI-containing therapy. Further experiments and surveillance are needed in patients treated with NNRTI(s) as well as NRTIs.

Mutations at multiple residues are present in the MDR variants of the Q151M and the fingers insertion complexes. Q151M complexes typically contain at least four mutations, including V75I, F77L, and F116Y in addition to Q151M (21). Insertion complexes generally contain an insertion of six bases that code for two amino acids in the background of the classical AZT resistance backbone such as T215Y (41). These results suggest that genetic barriers to developing these MDR mutations appear to be high, consistent with their low incidence (35). Genetic barriers to the G333D/E complex also seem to be high, since G333D/E requires other TAMs to develop this certain resistance phenotype (7). In contrast, a single nucleotide substitution (AAT to ATT) is sufficient to develop the N348I mutation, indicating that the genetic barrier to N348I is low. This may contribute to an increased prevalence of N348I during prolonged chemotherapy with AZT and/or ddI.

The disappearance of N348I was relatively rapid following interruption of treatment (Fig. 1 and Table 5). This was consistent with the observed replication kinetics of N348I HIV-1 where strong impairment was observed in MT-2 and SupT1 cells (Fig. 2). However, in PM1 cells and PHA-stimulated PBMCs, this reduction was moderate, and in H9 cells little reduction was observed. Since both PM1 and H9 cells were originally derived from the same T-cell line, Hut78 (25, 26), some properties for HIV replication may be identical. Availability of deoxynucleoside triphosphates or some cellular factors may compensate the effect of N348I on RT activity, suggesting that some cell populations in patients might harbor HIV-1 with N348I due to its comparable replication kinetics with the WT.

How might the N348I mutation affect resistance to NRTI and NNRTI inhibitors that act with entirely different mechanisms and target different binding sites? Theoretically, it is possible that the N348I mutation at either p66 or p51 or both subunits is responsible for the resistance phenotype. It is also possible that NRTI and NNRTI resistance do not involve the same subunit. However, the N348I mutation in p51 is 50 to 60 Å away from the polymerase active site and the NNRTI binding pocket where the affected inhibitors are expected to bind. Similarly, the mutation site in p51 is 15 to 20 Å away from the interface of the two subunits or the DNA binding cleft. Meanwhile, the mutation site in the p66 subunit is close to the NNRTI-binding pocket and the nucleic acid binding cleft. Hence, it is more likely that the effects of the N348I mutation

are mediated through the p66 subunit mutation, although an involvement of the mutation at the p51 subunit currently cannot be ruled out and should be addressed by biochemical experiments.

In terms of NNRTI resistance, our molecular modeling analysis is consistent with a hypothesis that the mutation is likely to affect the flexibility and mobility of the p66 thumb subdomain. Extensive crystallographic work with HIV-1 RT in several forms, including an unliganded form, in complex with DNA substrates or NNRTIs has revealed that during the course of DNA polymerization, the p66 thumb subdomain undergoes major conformational motions that are critical for efficient catalysis. Alignment of multiple structures of HIV RT suggests that the p66 thumb moves as a rigid body with its base hinged to the palm subdomain exactly near residue 348 (Fig. 3). Residue 348 is proximal to, and likely to affect, the relative interactions between residues of the p66 connection (T351) and p66 thumb subdomains (V317, I270, P272, W239, and eventually Y318). The proximity of residue 348 to this hinge region leads us to believe that changes imparted by the N348I mutation alter the mobility and flexibility of the thumb subdomain. Subtle changes in the interactions between V317 and N348 may also reposition W239 and its neighboring Y318 in the NNRTI-binding pocket. Interestingly, the Y318F mutation affects NNRTI resistance in a similar way as N348I: it decreases susceptibility to NVP and DLV but not to EFV (19, 33). Biochemical binding experiments of RTs with NNRTIs would directly evaluate this hypothesis.

The effect of the N348I mutation on NRTI resistance cannot be rationalized by direct interactions of the mutated residue with the NRTI binding site. It is tempting to speculate that minor changes in the p66 thumb subdomain hinge motions also have minor effects on the positioning of the nucleic acid, which in turn affects the ability to discriminate between NRTI and the normal substrate by an as yet undefined mechanism. However, direct biochemical experimental evidence will be needed to determine the precise molecular details of the specific mechanisms of NRTI resistance.

It has been proposed previously that an imbalance between reverse transcription and RNA degradation plays an important role in NRTI resistance (25). Pathak and colleagues proposed that connection subdomain mutations may result in a slower RNase H reaction, and this in turn may provide an increased time period available for AZT excision, especially with TAMs (28–30). In the case of N348I, Yap et al. recently reported that N348I decreases RNase H enzymatic activity (42). At present, available evidence is consistent with a model in which these connection subdomain mutations alter the affinity of the RT for template/primer, enhance nucleoside excision, and reduce template switching.

Several studies, including recent work by Delviks-Frankenberry et al. and Brehm et al. (4, 11), highlighted the necessity to expand sequencing analysis to include the connection and RNase H subdomains. This contention is further supported by results in this work and by others (16, 28, 42, 43) showing that mutations at the connection subdomain influence susceptibility to some antiretroviral drugs. Hence, there is a growing interest in obtaining genotypic information from expanded areas of RT that would be useful for a more complete analysis of HIV drug resistance. Interestingly, already two out of four commercially available genotypic and phenotypic assay kits are designed to include in their analysis at least part of the connection subdomain (Antivirogram by Virco up to RT residue 400 and ViroSeq by Abbott/Celera Diagnostics up to RT residue 335).

The present study identifies N348I as a MDR mutation in HIV-1 RT. This knowledge provides information that may be useful in designing more efficient therapeutic strategies that can improve clinical outcome and help prevent the emergence of MDR variants, especially in salvage therapy. This work further highlights the functional role of the HIV-1 RT connection subdomain in drug resistance. Future studies that focus on the structural and biochemical properties of connection subdomain RT mutants should reveal the molecular details of NRTI and NNRTI drug resistance caused by connection subdomain residues.

ACKNOWLEDGMENTS

This work was supported by a grant for the promotion of AIDS Research from the Ministry of Health, Labor and Welfare (to A.H., E.K., Y.S., M.M., H.G., M.T., and S.O.), a grant for Research for Health Sciences Focusing on Drug Innovation from The Japan Health Sciences Foundation (E.K and M.M), a grant from the Organization of Pharmaceutical Safety and Research (A.H., H.G., and S.O.) and a grant from the ministry of Education, Culture, Sports, Science, and Technology (E.K).

We thank Yukiko Takahashi and Fujie Negishi for sample preparation and the AIDS Clinical Center coordinator nurses for their dedicated assistance.

REFERENCES

1. **Antinori, A., M. Zaccarelli, A. Cingolani, F. Forbici, M. G. Rizzo, M. P. Trotta, S. Di Giambenedetto, P. Narciso, A. Ammassari, E. Girardi, A. De Luca, and C. F. Perno.** 2002. Cross-resistance among nonnucleoside reverse transcriptase inhibitors limits recycling efavirenz after nevirapine failure. AIDS Res. Hum. Retrovir. **18**:835–838.
2. **Baldanti, F., S. Paolucci, G. Maga, N. Labo, U. Hubscher, A. Y. Skoblov, L. Victorova, S. Spadari, L. Minoli, and G. Gerna.** 2003. Nevirapine-selected mutations Y181I/C of HIV-1 reverse transcriptase confer cross-resistance to stavudine. AIDS **17**:1568–1570.
3. **Boyer, P. L., S. G. Sarafianos, E. Arnold, and S. H. Hughes.** 2002. Nucleoside analog resistance caused by insertions in the fingers of human immunodeficiency virus type 1 reverse transcriptase involves ATP-mediated excision. J. Virol. **76**:9143–9151.
4. **Brehm, J. H., D. Koontz, J. D. Meteer, V. Pathak, N. Sluis-Cremer, and J. W. Mellors.** 2007. Selection of mutations in the connection and RNase H domains of human immunodeficiency virus type 1 reverse transcriptase that increase resistance to 3′-azido-3′-dideoxythymidine. J. Virol. **81**:7852–7859.
5. **Brenner, B., D. Turner, M. Oliveira, D. Moisi, M. Detorio, M. Carobene, R. G. Marlink, J. Schapiro, M. Roger, and M. A. Wainberg.** 2003. A V106M mutation in HIV-1 clade C viruses exposed to efavirenz confers cross-resistance to non-nucleoside reverse transcriptase inhibitors. AIDS **17**:F1–5.
6. **Brown, A. J., H. M. Precious, J. M. Whitcomb, J. K. Wong, M. Quigg, W. Huang, E. S. Daar, R. T. D'Aquila, P. H. Keiser, E. Connick, N. S. Hellmann, C. J. Petropoulos, D. D. Richman, and S. J. Little.** 2000. Reduced susceptibility of human immunodeficiency virus type 1 (HIV-1) from patients with primary HIV infection to nonnucleoside reverse transcriptase inhibitors is associated with variation at novel amino acid sites. J. Virol. **74**:10269–10273.
7. **Caride, E., R. Brindeiro, K. Hertogs, B. Larder, P. Dehertogh, E. Machado, C. A. de Sa, W. A. Eyer-Silva, F. S. Sion, L. F. Passioni, J. A. Menezes, A. R. Calazans, and A. Tanuri.** 2000. Drug-resistant reverse transcriptase genotyping and phenotyping of B and non-B subtypes (F and A) of human immunodeficiency virus type I found in Brazilian patients failing HAART. Virology **275**:107–115.
8. **Cherrington, J. M., A. S. Mulato, M. D. Fuller, and M. S. Chen.** 1996. Novel mutation (K70E) in human immunodeficiency virus type 1 reverse transcriptase confers decreased susceptibility to 9-[2-(phosphonomethoxy)ethyl]adenine in vitro. Antimicrob. Agents Chemother. **40**:2212–2216.
9. **Das, K., S. G. Sarafianos, A. D. Clark, Jr., P. L. Boyer, S. H. Hughes, and E. Arnold.** 2007. Crystal structures of clinically relevant Lys103Asn/Tyr181Cys double mutant HIV-1 reverse transcriptase in complexes with ATP and non-nucleoside inhibitor HBY 097. J. Mol. Biol. **365**:77–89.
10. **de Jong, J. J., J. Goudsmit, V. V. Lukashov, M. E. Hillebrand, E. Baan, R. Huismans, S. A. Danner, J. H. ten Veen, F. de Wolf, and S. Jurriaans.** 1999.

Insertion of two amino acids combined with changes in reverse transcriptase containing tyrosine-215 of HIV-1 resistant to multiple nucleoside analogs. AIDS **13:**75–80.

11. **Delviks-Frankenberry, K. A., G. N. Nikolenko, R. Barr, and V. K. Pathak.** 2007. Mutations in human immunodeficiency virus type 1 RNase H primer grip enhance 3′-azido-3′-deoxythymidine resistance. J. Virol. **81:**6837–6845.
12. **Esnouf, R., J. Ren, C. Ross, Y. Jones, D. Stammers, and D. Stuart.** 1995. Mechanism of inhibition of HIV-1 reverse transcriptase by non-nucleoside inhibitors. Nat. Struct. Biol. **2:**303–308.
13. **Gatanaga, H., S. Oka, S. Ida, T. Wakabayashi, T. Shioda, and A. Iwamoto.** 1999. Active HIV-1 redistribution and replication in the brain with HIV encephalitis. Arch. Virol. **144:**29–43.
14. **Hachiya, A., S. Aizawa-Matsuoka, M. Tanaka, Y. Takahashi, S. Ida, H. Gatanaga, Y. Hirabayashi, A. Kojima, M. Tatsumi, and S. Oka.** 2001. Rapid and simple phenotypic assay for drug susceptibility of human immunodeficiency virus type 1 using CCR5-expressing HeLa/CD4$^+$ cell clone 1–10 (MAGIC-5). Antimicrob. Agents Chemother. **45:**495–501.
15. **Hachiya, A., H. Gatanaga, E. Kodama, M. Ikeuchi, M. Matsuoka, S. Harada, H. Mitsuya, S. Kimura, and S. Oka.** 2004. Novel patterns of nevirapine resistance-associated mutations of human immunodeficiency virus type 1 in treatment-naive patients. Virology **327:**215–224.
16. **Hachiya, A., E. Kodama, S. G. Sarafianos, M. M. Schuckman, M. Matsuoka, M. Takiguchi, G. Gatanaga, and S. Oka.** 2007. A novel mutation, N348I in HIV-1 reverse transcriptase induced by NRTI treatment, confers nevirapine resistance, abstr. 593. Abstr. 14th Conf. Retrovir. Opportunistic Infect., Los Angels, CA.
17. **Hammer, S. M., M. S. Saag, M. Schechter, J. S. Montaner, R. T. Schooley, D. M. Jacobsen, M. A. Thompson, C. C. Carpenter, M. A. Fischl, B. G. Gazzard, J. M. Gatell, M. S. Hirsch, D. A. Katzenstein, D. D. Richman, S. Vella, P. G. Yeni, and P. A. Volberding.** 2006. Treatment for adult HIV infection: 2006 recommendations of the International AIDS Society-USA panel. JAMA **296:**827–843.
18. **Hammond, J. L., U. M. Parikh, D. L. Koontz, S. Schlueter-Wirtz, C. K. Chu, H. Z. Bazmi, R. F. Schinazi, and J. W. Mellors.** 2005. In vitro selection and analysis of human immunodeficiency virus type 1 resistant to derivatives of beta-2′,3′-didehydro-2′,3′-dideoxy-5-fluorocytidine. Antimicrob. Agents Chemother. **49:**3930–3932.
19. **Harrigan, P. R., M. Salim, D. K. Stammers, B. Wynhoven, Z. L. Brumme, P. McKenna, B. Larder, and S. D. Kemp.** 2002. A mutation in the 3′ region of the human immunodeficiency virus type 1 reverse transcriptase (Y318F) associated with nonnucleoside reverse transcriptase inhibitor resistance. J. Virol. **76:**6836–6840.
20. **Huang, H., R. Chopra, G. L. Verdine, and S. C. Harrison.** 1998. Structure of a covalently trapped catalytic complex of HIV-1 reverse transcriptase: implications for drug resistance. Science **282:**1669–1675.
21. **Kavlick, M. F., K. Wyvill, R. Yarchoan, and H. Mitsuya.** 1998. Emergence of multi-dideoxynucleoside-resistant human immunodeficiency virus type 1 variants, viral sequence variation, and disease progression in patients receiving antiretroviral chemotherapy. J. Infect. Dis. **177:**1506–1513.
22. **Kemp, S. D., C. Shi, S. Bloor, P. R. Harrigan, J. W. Mellors, and B. A. Larder.** 1998. A novel polymorphism at codon 333 of human immunodeficiency virus type 1 reverse transcriptase can facilitate dual resistance to zidovudine and L-2′,3′-dideoxy-3′-thiacytidine. J. Virol. **72:**5093–5098.
23. **Kodama, E. I., S. Kohgo, K. Kitano, H. Machida, H. Gatanaga, S. Shigeta, M. Matsuoka, H. Ohrui, and H. Mitsuya.** 2001. 4′-Ethynyl nucleoside analogs: potent inhibitors of multidrug-resistant human immunodeficiency virus variants in vitro. Antimicrob. Agents Chemother. **45:**1539–1546.
24. **Larder, B. A., S. D. Kemp, and P. R. Harrigan.** 1995. Potential mechanism for sustained antiretroviral efficacy of AZT-3TC combination therapy. Science **269:**696–699.
25. **Lusso, P., F. Cocchi, C. Balotta, P. D. Markham, A. Louie, P. Farci, R. Pal, R. C. Gallo, and M. S. Reitz, Jr.** 1995. Growth of macrophage-tropic and primary human immunodeficiency virus type 1 (HIV-1) isolates in a unique CD4$^+$ T-cell clone (PM1): failure to downregulate CD4 and to interfere with cell-line-tropic HIV-1. J. Virol. **69:**3712–3720.
26. **Mann, D. L., S. J. O'Brien, D. A. Gilbert, Y. Reid, M. Popovic, E. Read-Connole, R. C. Gallo, and A. F. Gazdar.** 1989. Origin of the HIV-susceptible human CD4$^+$ cell line H9. AIDS Res. Hum. Retrovir. **5:**253–255.
27. **Nameki, D., E. Kodama, M. Ikeuchi, N. Mabuchi, A. Otaka, H. Tamamura, M. Ohno, N. Fujii, and M. Matsuoka.** 2005. Mutations conferring resistance to human immunodeficiency virus type 1 fusion inhibitors are restricted by gp41 and Rev-responsive element functions. J. Virol. **79:**764–770.
28. **Nikolenko, G. N., K. A. Delviks-Frankenberry, S. Palmer, F. Maldarelli, M. J. Fivash, Jr., J. M. Coffin, and V. K. Pathak.** 2007. Mutations in the connection domain of HIV-1 reverse transcriptase increase 3′-azido-3′-deoxythymidine resistance. Proc. Natl. Acad. Sci. USA **104:**317–322.
29. **Nikolenko, G. N., S. Palmer, F. Maldarelli, J. W. Mellors, J. M. Coffin, and V. K. Pathak.** 2005. Mechanism for nucleoside analog-mediated abrogation of HIV-1 replication: balance between RNase H activity and nucleotide excision. Proc. Natl. Acad. Sci. USA **102:**2093–2098.
30. **Nikolenko, G. N., E. S. Svarovskaia, K. A. Delviks, and V. K. Pathak.** 2004. Antiretroviral drug resistance mutations in human immunodeficiency virus type 1 reverse transcriptase increase template-switching frequency. J. Virol. **78:**8761–8770.
31. **Paolucci, S., F. Baldanti, G. Maga, R. Cancio, M. Zazzi, M. Zavattoni, A. Chiesa, S. Spadari, and G. Gerna.** 2004. Gln145Met/Leu changes in human immunodeficiency virus type 1 reverse transcriptase confer resistance to nucleoside and nonnucleoside analogs and impair virus replication. Antimicrob. Agents Chemother. **48:**4611–4617.
32. **Paolucci, S., F. Baldanti, M. Tinelli, G. Maga, and G. Gerna.** 2003. Detection of a new HIV-1 reverse transcriptase mutation (Q145M) conferring resistance to nucleoside and non-nucleoside inhibitors in a patient failing highly active antiretroviral therapy. AIDS **17:**924–927.
33. **Pelemans, H., R. M. Esnouf, H. Jonckheere, E. De Clercq, and J. Balzarini.** 1998. Mutational analysis of Tyr-318 within the non-nucleoside reverse transcriptase inhibitor binding pocket of human immunodeficiency virus type I reverse transcriptase. J. Biol. Chem. **273:**34234–34239.
34. **Ren, J., L. E. Bird, P. P. Chamberlain, G. B. Stewart-Jones, D. I. Stuart, and D. K. Stammers.** 2002. Structure of HIV-2 reverse transcriptase at 2.35-Å resolution and the mechanism of resistance to non-nucleoside inhibitors. Proc. Natl. Acad. Sci. USA **99:**14410–14415.
35. **Rhee, S. Y., W. J. Fessel, A. R. Zolopa, L. Hurley, T. Liu, J. Taylor, D. P. Nguyen, S. Slome, D. Klein, M. Horberg, J. Flamm, S. Follansbee, J. M. Schapiro, and R. W. Shafer.** 2005. HIV-1 Protease and reverse-transcriptase mutations: correlations with antiretroviral therapy in subtype B isolates and implications for drug-resistance surveillance. J. Infect. Dis. **192:**456–465.
36. **Sarafianos, S. G., K. Das, C. Tantillo, A. D. Clark, Jr., J. Ding, J. M. Whitcomb, P. L. Boyer, S. H. Hughes, and E. Arnold.** 2001. Crystal structure of HIV-1 reverse transcriptase in complex with a polypurine tract RNA: DNA. EMBO J. **20:**1449–1461.
37. **Shafer, R. W., S. Y. Rhee, D. Pillay, V. Miller, P. Sandstrom, J. M. Schapiro, D. R. Kuritzkes, and D. Bennett.** 2007. HIV-1 protease and reverse transcriptase mutations for drug resistance surveillance. AIDS **21:**215–223.
38. **Shirasaka, T., M. F. Kavlick, T. Ueno, W. Y. Gao, E. Kojima, M. L. Alcaide, S. Chokekijchai, B. M. Roy, E. Arnold, and R. Yarchoan.** 1995. Emergence of human immunodeficiency virus type 1 variants with resistance to multiple dideoxynucleosides in patients receiving therapy with dideoxynucleosides. Proc. Natl. Acad. Sci. USA **92:**2398–2402.
39. **Sluis-Cremer, N., C. W. Sheen, S. Zelina, P. S. Torres, U. M. Parikh, and J. W. Mellors.** 2007. Molecular mechanism by which the K70E mutation in human immunodeficiency virus type 1 reverse transcriptase confers resistance to nucleoside reverse transcriptase inhibitors. Antimicrob. Agents Chemother. **51:**48–53.
40. **Tuske, S., S. G. Sarafianos, A. D. Clark, Jr., J. Ding, L. K. Naeger, K. L. White, M. D. Miller, C. S. Gibbs, P. L. Boyer, P. Clark, G. Wang, B. L. Gaffney, R. A. Jones, D. M. Jerina, S. H. Hughes, and E. Arnold.** 2004. Structures of HIV-1 RT-DNA complexes before and after incorporation of the anti-AIDS drug tenofovir. Nat. Struct. Mol. Biol. **11:**469–474.
41. **Winters, M. A., K. L. Coolley, Y. A. Girard, D. J. Levee, H. Hamdan, R. W. Shafer, D. A. Katzenstein, and T. C. Merigan.** 1998. A 6-base pair insert in the reverse transcriptase gene of human immunodeficiency virus type 1 confers resistance to multiple nucleoside inhibitors. J. Clin. Investig. **102:**1769–1775.
42. **Yap, S. H., C. W. Sheen, J. Fahey, M. Zanin, D. Tyssen, V. D. Lima, B. Wynhoven, M. Kuiper, N. Sluis-Cremer, P. R. Harrigan, and G. Tachedjian.** 2007. N348I in the connection domain of HIV-1 reverse transcriptase confers zidovudine and nevirapine resistance. PLoS Med. **4:**e335.
43. **Yap, S. H., B. Wynhoven, M. Kuiper, C. W. Sheen, N. Sluis-Cremer, R. Harrigan, and G. Tachedjian.** 2007. A mutation in the connection subdomain of the HIV-1 reverse transcriptase (N348I) is selected commonly in vivo and confers decreased susceptibility to zidovudine and nevirapine, abstr. 594. Abstr. 14th Conf. Retrovir. Opportunistic Infect., Los Angels, CA.